

Cross-Study Replicability in Cluster Analysis

Lorenzo Masoero^{*}, Emma Thomas¹, Giovanni Parmigiani², Svitlana Tyekucheva², and Lorenzo Trippa²

^{*}*Email address:* lo.masoero@gmail.com

¹*Department of Biostatistics, Harvard T.H. Chan School of Public Health*

²*Department of Data Science, DFCI*

September 10, 2022

1 Introduction

Clustering, the task of partitioning data into distinct classes, is fundamental in a variety of fields and applications. For example, in genomics, clustering procedures are used for exploratory analyses, dimensionality reduction and to identify interpretable groups within high-dimensional data, such as gene expression studies.

One of the difficulties in clustering, common to other techniques in unsupervised learning, is the ambiguity of the notion of success. In contrast to supervised learning, where ground truth measurements can be used to validate the performance of a learning procedure (e.g., the precision of a classifier), in unsupervised learning a direct measure of success is not available. In applications it is however crucial to identify criteria to assess the reliability of these unsupervised learning methods.

In this paper we examine the problem of quantifying the quality of cluster analyses through the lens of replicability. We consider as a motivating example clustering in gene expression studies aiming to identify cancer subtypes. In this context, a dataset is a high dimensional collection of gene expression profiles of different patients, and clustering analyses try to identify biologically relevant groups of observations. An ideal cluster analysis identifies cancer subtypes and in turn allows scientists to develop specific and effective treatment strategies for the different subtypes.

We introduce notation and relevant background in Section 2, where we provide a thorough review of the existing literature on clustering replicability. Next, in Section 3, we focus on the assessment of clustering replicability when multiple sources of data are available — a question of increasing importance in biosciences, where collections of datasets generated by different research groups and institutions are often available [Hayes et al., 2006, Bernau et al., 2014, Trippa et al., 2015, National Academies of Sciences and Medicine, 2019]. We develop a

novel method that can help understand whether cluster procedures ran across multiple datasets are replicable. The idea underlying the replicability metrics we employ is that clusters consistently identified by independent analyses of distinct datasets can be used as a criterion to assess the replicability of the analysis. We show how to generate replicability summaries, representative of the similarity of the groups identified by a clustering method across independent analyses of the available datasets. Our procedure evaluates the replicability, without constraints on the choice of the clustering method, and across any number of datasets, at both a *global* scale, that is for the whole data collection, as well as at a *local* scale, that is for an individual cluster. We test our method on synthetic data in Section 4, and we present an application in cancer research in Section 5. We provide additional experiments, also using competing replicability methods in the Appendix. Code to replicate all our experiments can be found at https://github.com/lorenzomasoero/clustering_replicability.

2 Clustering Replicability in a Single Study

With the growth of high dimensional and multi-modal datasets in several areas of science, practitioners need replicable procedures to analyze and simplify their data. In biological sciences, for example, advances in data-collection technologies allow investigators to study increasingly complex datasets, with large sample sizes and feature lists (gene expression profiles, demographics, imaging). While these rich datasets come with the promise of providing new insights, they also present practical challenges. Analysts often need dimensionality reduction techniques to visualize and explore the data. In this context, clustering algorithms have emerged as a preeminent technique because of their scalability, ease-of-use and wide applicability. While several clustering algorithms are available, assessing the usefulness and quality of the results they produce is a difficult problem, which has received considerable interest in the literature. In this section, we focus on replicability of cluster analyses and review important recent contributions in the literature on this problem.

2.1 Preliminaries and notation

Data A dataset $\mathbf{X} = \{x_1, \dots, x_n\}$ is an unordered collection of datapoints. An individual observation or datapoint $x_i = [x_{i,1}, \dots, x_{i,p}]$ is a p -dimensional vector, e.g., the gene expression profile of patient i , where $x_{i,r}$ is the expression level of the r -th gene of interest.

Clustering Algorithms A clustering algorithm \mathcal{A} is a procedure that takes as input a dataset \mathbf{X} and outputs a “learned” clustering function $\psi(\cdot; \mathcal{A}, \mathbf{X}) : \mathbb{R}^p \rightarrow [k] := \{1, 2, \dots, k\}$. Notice that $\psi(\cdot; \mathcal{A}, \mathbf{X})$ maps *any* point $y \in \mathbb{R}^p$ to a class $\ell \in [k]$.

Partitioning via Clustering Functions Recall that subsets U_1, \dots, U_k s.t. $U_j \cap U_\ell = \emptyset$ for $j \neq \ell$ and $\cup_{j=1}^k U_j = \mathbf{X}'$ form a partition of \mathbf{X}' . Given clustering algorithm \mathcal{A} and training dataset \mathbf{X} , a partition of *any* collection of data points \mathbf{X}' can be directly obtained by applying the learned clustering function $\psi(\cdot; \mathcal{A}, \mathbf{X})$ to all points $x' \in \mathbf{X}'$. Datapoints in \mathbf{X}' sharing the same cluster label belong to the same subset of the partition, e.g. the j -th subset is given by $U_j = \{x' \in \mathbf{X}' : \psi(x'; \mathcal{A}, \mathbf{X}) = j\}$. We let $\Psi(\mathbf{X}'; \mathcal{A}, \mathbf{X}) := \{\psi(x'; \mathcal{A}, \mathbf{X}), x' \in \mathbf{X}'\}$ denote the labels of datapoints in \mathbf{X}' induced by the clustering function $\psi(\cdot; \mathcal{A}, \mathbf{X})$. In what follows, we write $\psi(\cdot)$ or $\psi(\cdot; \mathbf{X})$ in place of $\psi(\cdot; \mathcal{A}, \mathbf{X})$ and $\Psi(\cdot)$ or $\Psi(\cdot; \mathbf{X})$ in place of $\Psi(\cdot; \mathcal{A}, \mathbf{X})$ when \mathcal{A}, \mathbf{X} are clear from the context.

Binary Partitions For $y, w \in \mathbb{R}^p$ and a clustering function $\psi(\cdot; \mathcal{A}, \mathbf{X})$, we define the co-clustering operator $\psi_w(y; \mathcal{A}, \mathbf{X}) = \mathbb{1}\{\psi(y; \mathcal{A}, \mathbf{X}) = \psi(w; \mathcal{A}, \mathbf{X})\}$.

Example: k -means Let \mathcal{A} be the k -means algorithm. Given a training dataset \mathbf{X} , this algorithm works by approximately solving the optimization problem:

$$\min_{U_1, \dots, U_k} \sum_{\ell=1}^k \sum_{i \in U_\ell} \|x_i - c_\ell\|_2, \quad (1)$$

where U_1, \dots, U_k are the disjoint subsets forming a partition of \mathbf{X} , and for $\ell = 1, \dots, k$, $c_\ell = [c_{\ell,1}, \dots, c_{\ell,p}]$ is the ℓ -th ‘‘centroid’’ of U_ℓ , with components $c_{\ell,r} = (\sum_{i \in U_\ell} x_{i,r}) / |U_\ell| \in \mathbb{R}$, $r \in [p]$. Here, we view k -means as the procedure that learns the clustering function

$$\psi(x'; \mathcal{A}, \mathbf{X}) = \arg \min_{\ell \in \{1, \dots, k\}} \|x' - c_\ell\|_2. \quad (2)$$

Remark: Induced Clustering Functions In some cases, the output of a clustering algorithm is not a clustering function, rather simply a partition of the training set (e.g. as in hierarchical clustering). In these cases we obtain a clustering function indirectly, via an additional classification step. In the present work, for this class of algorithms, we adopt a nearest neighbor approach (although other classifiers could be used): let $z(i) \in [k]$ be the cluster label for datapoint x_i , $i = 1, \dots, n$ obtained by applying \mathcal{A} to \mathbf{X} . Then, for a generic $y \in \mathbb{R}^p$, and $d(\cdot, \cdot)$ a distance metric on \mathbb{R}^p , we let $\psi(y) := z(\arg \min_{x_i \in \mathbf{X}} d(y, x_i))$.

2.2 Clustering Replicability via Stability

Having introduced the necessary notation, we now start out review existing methods in the literature which make use of replicability to assess the quality of clustering analyses.

One of the most important paradigms for the replicability of the analysis of complex, high-dimensional data follows under the notion of statistical stability [Yu, 2013, Lim and Yu, 2016, Murdoch et al., 2019, Arrieta et al., 2020]. Namely,

the idea that a statistical analysis is replicable if it stable, i.e. it produces similar results when performed several times, using the same or slightly different data. Here, we discuss stability in the context of clustering analyses.

2.2.1 Global Replicability

A simple measure of clustering replicability can be obtained by comparing the partitions learned over multiple repetitions of algorithm \mathcal{A} on the same dataset \mathbf{X} . If \mathcal{A} is stable, it should produce the same output when re-run on the same input. Let $\psi^{(1)}, \psi^{(2)}$ be the two clustering functions learned by running \mathcal{A} twice on dataset \mathbf{X} . It is possible that, even when repeatedly applied to the same dataset, multiple runs give raise to different results. E.g., if \mathcal{A} is k -means, distinct initializations — potentially randomly selected — may lead to different local minima of the objective function in Equation (1). This allows to think of ψ as a random element. Building on this idea, one can measure cluster replicability of \mathcal{A} by employing a measure of discrepancy or distance between the partitions of \mathbf{X} induced by $\psi^{(1)}$ and $\psi^{(2)}$. In this spirit, Von Luxburg [2010] suggested using the minimal matching distance, defined as the minimum number of labels switches needed to make the partitions induced by $\psi^{(1)}$ and $\psi^{(2)}$ identical:

$$\min_{\pi} \sum_{i=1}^n \mathbb{1} \left[\psi^{(1)}(x_i) \neq \pi \left\{ \psi^{(2)}(x_i) \right\} \right], \quad (3)$$

where π is a permutation of the k labels of the clusters. Notice that, while in this example we focused on k -means, the same argument could be applied to any other clustering algorithm (e.g., hierarchical clustering, or even regression-based clustering), by virtue of our remark on “Induced Clustering Functions” above.

A clustering algorithm could produce the same output when re-applied to the same dataset, but its output might change considerably if we just slightly change the input data. Several authors have therefore generalized the definition of stability by comparing the results of an algorithm applied to slightly different versions of the same dataset [Bryan, 2004, Lange et al., 2004, Ben-David et al., 2007]. This notion of clustering stability is widely accepted among practitioners, since a replicable clustering procedure should not be too sensitive to small perturbations of the data. Standard approaches to produce perturbed versions of the original dataset and to perform stability analyses include (i) sub sampling the data [Levine and Domany, 2001], or (ii) corrupting individual datapoints, e.g. by adding random noise [Hennig, 2007]. If the results obtained by performing clustering on the corrupted datasets are similar to the ones obtained on the original data, then the cluster analysis is stable. Instead, when the results differ across perturbed datasets — despite the fact that the datasets are similar by construction — the clustering algorithm is deemed unstable.

A general stability-based measure of clustering replicability on dataset \mathbf{X} is then as follows. Let B be a large integer. For $b = 1, \dots, B$ let $\mathbf{X}^{(b)}$ be either (i) a random subsample of \mathbf{X} (e.g., a draw of $n' < n$ datapoints without replacement), (ii) a corrupted version of \mathbf{X} , in which the i -th datapoint $x_i^{(b)} = x_i + \epsilon_i^{(b)}$, where

$\epsilon_i^{(b)}$ is a random error term or (iii) a combination of (i) and (ii). A stability measure is obtained by averaging the minimal matching distance of Equation (3) between the partition of \mathbf{X} learned using the full dataset and the partition obtained with the b -th corrupted dataset,

$$B^{-1} \sum_{b=1}^B d \left\{ \Psi(\mathbf{X}; \mathcal{A}, \mathbf{X}); \Psi(\mathbf{X}; \mathcal{A}, \mathbf{X}^{(b)}) \right\}.$$

2.2.2 Local Replicability

Besides assessing the global replicability of a clustering algorithm, scientists might be interested in understanding the local replicability of a specific cluster of interest, e.g. because this cluster is hypothesized to be biologically relevant. To do so, Smolkin and Ghosh [2003] propose the following procedure: run a clustering algorithm on \mathbf{X} and let U_1, \dots, U_k be the clusters identified. Given a fraction $\alpha \in (p^{-1}, 1]$ and a large integer value B , for $b = 1, \dots, B$, select a random subset of $p' = \lfloor \alpha p \rfloor$ covariates from the p original ones. Let $\mathbf{X}^{(b)}$ be the dataset obtained by retaining for every datapoint only the $p' < p$ randomly selected covariates. Perform the same clustering procedure as before, but now on $\mathbf{X}^{(b)}$, and let $U_1^{(b)}, \dots, U_k^{(b)}$ be the resulting clusters. Stability of the j -th cluster U_j is measured by the fraction of repetitions for which there exists a cluster $U_\ell^{(b)}$ such that $U_j \subseteq U_\ell^{(b)}$:

$$\frac{1}{B} \sum_{b=1}^B \mathbb{1} \left(\sum_{\ell=1}^k \mathbb{1}(U_j \subseteq U_\ell^{(b)}) > 0 \right).$$

Variations of this methods and similar ideas have also been proposed. E.g. Hennig [2007] uses the Jaccard coefficient: $\frac{1}{B} \sum_{b=1}^B \max_{i=1, \dots, k} \frac{|U_j \cap U_i^{(b)}|}{|U_j \cup U_i^{(b)}|}$. In either case, the mean across re-runs could be replaced by other summaries, such as the median or quantiles.

In another notable approach, McShane et al. [2002] propose two metrics for local clustering stability, the R -index and the D -index. The method relies on considering again B perturbations $\mathbf{X}^{(1)}, \dots, \mathbf{X}^{(B)}$ of the original dataset \mathbf{X} , with $\mathbf{X}^{(b)} = \{x_1 + e_1^{(b)}, \dots, x_n + e_n^{(b)}\}$, where $e_i^{(b)}$ are i.i.d. mean-zero Gaussian error terms with variance adequately chosen for the data under consideration. For U_j a cluster of interest in \mathbf{X} , the R -index quantifies U_j 's stability by computing the average fraction of pairs of datapoints in U_j which remains clustered together after re-clustering the perturbed dataset $\mathbf{X}^{(b)}$ across re-runs. The D -index computes across re-runs the average number of ‘‘discrepancies’’ (additions or deletions) between U_j and the cluster with the highest overlap in $\mathbf{X}^{(b)}$.

2.3 Cluster Analyses and Prediction Accuracy

2.3.1 Global Replicability

A different approach for clustering replicability is driven by the idea of prediction accuracy, where concepts developed in the context of classification are adapted to clustering. In influential work Tibshirani and Walther [2005] relied on the idea of prediction accuracy to develop a procedure for identifying the “best” clustering algorithm \mathcal{A} for the data at hand. In a nutshell, the “best” algorithm is the one that allows to predict with the highest accuracy clustering co-membership of points in a test set, using a clustering function learned on a training set. More precisely, first split the data into a training and test dataset $\mathbf{X} = \{x_1, \dots, x_n\}$, $\mathbf{X}' = \{x'_1, \dots, x'_m\}$. Here, for simplicity, assume that \mathcal{A} identifies k clusters. Then,

- Run \mathcal{A} on \mathbf{X} and on \mathbf{X}' separately. Let U_1, \dots, U_k denote the subsets of the partition of \mathbf{X}' induced by $\Psi(\mathbf{X}'; \mathcal{A}, \mathbf{X}')$, and $m_j = |U_j|$, the size of subset j .
- Quantify the “prediction strength” by computing co-clustering occurrences: for any two points in the test set belonging to the same cluster, $x'_i, x'_\ell \in U_j$, let $\eta(x'_i, x'_j) = \mathbb{1} \{ \psi(x'_i; \mathcal{A}, \mathbf{X}) = \psi(x'_\ell; \mathcal{A}, \mathbf{X}) \}$. The prediction strength is defined as

$$\text{ps}(k) := \min_{1 \leq j \leq k} \left[\frac{\sum_{x'_i, x'_\ell \in U_j, i \neq \ell} \eta(x'_i, x'_j)}{m_j(m_j - 1)} \right]. \quad (4)$$

The authors use prediction strength to identify the number of clusters k into which the dataset should be partitioned — namely, letting be $k = \arg \max_{k' \geq 2} \text{ps}(k')$.

2.3.2 Local Replicability

Relatedly, Kapp and Tibshirani [2006] developed a cluster-specific measure of replicability, the “in-group-proportion” [IGP]. For a given cluster U_j , the IGP is the fraction of datapoints in U_j whose nearest neighbors are also in the same group: let $\text{nn}(x_i) = \arg \min_{x' \in \mathbf{X}} d(x_i, x')$, for a distance $d(\cdot, \cdot)$. Then,

$$\text{IGP}(U_j) = \frac{1}{|U_j|} \sum_{x_i \in U_j} \mathbb{1}[\text{nn}(x_i) \in U_j].$$

This measure can be used to assess the replicability of an individual cluster U_j .

2.4 Analyses Based on Tests of Statistical Significance

Last we consider methods to assess cluster replicability via tests of statistical significance. At a high level, these work by building statistical tests for the “null” hypothesis H_0 that the data does not contain distinct clusters. Tests can provide evidence that the data includes two or more clusters by rejecting the

null hypothesis. Most tests for clustering replicability are parametric, i.e. they assume that under H_0 the data originates from a posited parametric model. The tests work by comparing the value of a relevant test statistic, computed using the observed data \mathbf{X} , to the distribution of the same statistic under the null hypothesis. If the value of the test statistic is sufficiently unlikely under the null, then H_0 is rejected. Following McShane et al. [2002], we now discuss a general recipe to assess replicability of clustering using statistical tests:

1. Let F_0 be a distribution from which data is drawn under H_0 (e.g., Gaussian).
2. Let $d_i = \min_{j \neq i} \|x_i - x_j\|^2$ be x_i 's nearest neighbor distance and $G_\star(v) = \sum_i \mathbb{1}(d_i \leq v)/n$ the cumulative density function (CDF) of d_1, \dots, d_n .
3. Generate a sequence of datasets from the null model, $\mathbf{X}^{(b)}$, for $b = 1, \dots, B$. For each simulated dataset, obtain the CDF of the nearest neighbor distances $G_b(\cdot)$. Under H_0 , G_\star, G_1, \dots, G_B are approximately identically distributed.
4. Compute for $b \in \{\star, 1, \dots, B\}$ the test statistics:

$$s_b = \int_0^\infty \left\{ G_b(y) - \frac{1}{B} \sum_{b' \neq b} G_{b'}(y) \right\}^2 dy.$$

Each s_b can be interpreted as the distance of $G_b(\cdot)$ from the average of the other CDFs, $\frac{1}{B} \sum_{b' \neq b} G_{b'}(\cdot)$.

5. Compare s_\star to s_1, \dots, s_B . Reject H_0 at confidence level α if s_\star is larger than the $100 \times (1 - \alpha)$ percentile of $s_b, b = 1, \dots, B$.

Other measures besides the nearest neighbor distance (step 2) and other test statistics (step 4) could be employed (see Levenstien et al. [2003], Alexe et al. [2006], Bertoni and Valentini [2007], Liu et al. [2008] for other approaches).

Available Software

Among existing software for clustering replicability, we recommend the *R* packages `clValid` [Brock et al., 2008] and `fpc` [Hennig, 2015], which support a few of the replicability indices discussed above. We provide code to generate and test all the replicability metrics discussed in Section 2. Experimental results for all the methods discussed are presented in Masoero et al. [2022b, Appendix B].

3 Clustering and Cross-Study Replicability

3.1 Challenges and Strategies for Cross-Study Clustering Replicability

Often, scientists interested in investigating replicability have access to *multiple* datasets, and want to understand replicability properties of their analyses *across*

these datasets. Different datasets can have their own specificity, for example because of different study designs or technical differences in the instrumentation used to measure the variables. Hence, high replicability scores within each study do not necessarily imply replicability across different studies. Nonetheless it is possible to make progress in the more challenging assessment of replicability across multiple studies by extending some of the principles reviewed in the previous section. Here we provide a guide for this extension, discussing how to leverage the ideas presented in Section 2 for quantifying cross-study clustering replicability when multiple studies are available, and for selecting clustering algorithms with better cross-study replicability properties compared to others. To get started, we need an operational definition for cross-study replicability. For simplicity, consider two datasets \mathbf{X}, \mathbf{X}' — the “training” and “testing” dataset respectively. These could be data from independent studies probing the same molecular features on patients with similar clinical conditions. Informally, we say that clustering algorithm \mathcal{A} is replicable across \mathbf{X} and \mathbf{X}' if it is able to learn similar clustering functions across these two studies. We quantify the similarity of the clustering functions learned on \mathbf{X} and \mathbf{X}' in an intuitive way, by measuring the differences between the partitions of \mathbf{X}' obtained by using the clustering functions learned by training \mathcal{A} on \mathbf{X} and on \mathbf{X}' respectively. That is, by computing $d(\Psi(\mathbf{X}'; \mathcal{A}, \mathbf{X}), \Psi(\mathbf{X}'; \mathcal{A}, \mathbf{X}'))$, where $d(\cdot, \cdot)$ is a metric of discrepancy between two partitions of the set \mathbf{X}' .

Notice that this setting is similar to what already discussed in Section 2.3: e.g., the prediction strength of Equation (4), is an example of a similarity metric on partitions. However, while in the discussion in Section 2.3 the train and test data are random subsamples from the same dataset, here we allow for \mathbf{X} and \mathbf{X}' to be different, independent datasets. As a consequence of that, differently from the case discussed in Section 2.3, we do not expect a priori $d(\cdot, \cdot)$ to be symmetric in its arguments.

In our discussion, we use cancer subtype validation as a motivating example: we consider multiple datasets of patients gene expressions, collected by different investigators. Replicability analysis will help us understand whether the clustering learned on the dataset collected by one investigator identifies cancer subtypes in a different dataset.

3.2 Useful Metrics for Clustering Replicability

A key ingredient to quantify cross-study replicability is the choice of discrepancy metric $d(\cdot, \cdot)$ between partitions. Several options exist in the literature [Albatineh et al., 2006, Vinh et al., 2010, Jaskowiak et al., 2014]. Here, we consider two metrics: the Rand index (RI, Rand [1971]) and the mutual information (MI). In what follows, let $\mathbf{U} = \{U_1, \dots, U_{k_1}\}$ and $\mathbf{V} = \{V_1, \dots, V_{k_2}\}$ denote two partitions of the set $\mathbf{X}' = \{x'_1, \dots, x'_m\}$, with $|\mathbf{U}| = k_1$ and $|\mathbf{V}| = k_2$, respectively.

The Rand Index [RI] The Rand index is a simple pair-counting discrepancy measure, obtained by computing the fraction of pairs of datapoints on which two partitions \mathbf{U} and \mathbf{V} of the same set \mathbf{X}' agree. Let $N_{0,0}$ denote the number

of pairs of points which belong to different subsets in both partitions, $N_{1,1}$ the number of pairs which belong to the same subset in both partitions, $N_{1,0}$ the number of pairs which belong to the same subset in partition \mathbf{U} , but are in different subsets in partition \mathbf{V} , and symmetrically $N_{0,1}$ the number of pairs belonging to different subsets in partition \mathbf{U} and to the same subset in partition \mathbf{V} . Because there are exactly $\binom{m}{2}$ pairs of points, and each pair of points falls in exactly one of these categories, it follows that

$$N_{0,0} + N_{0,1} + N_{1,0} + N_{1,1} = \binom{m}{2}.$$

The Rand index for partitions \mathbf{U} , \mathbf{V} of the set \mathbf{X}' is then defined as

$$\text{RI}(\mathbf{U}, \mathbf{V}) = \frac{N_{0,0} + N_{1,1}}{\sum_{i=0}^1 \sum_{j=0}^1 N_{i,j}} = \frac{N_{0,0} + N_{1,1}}{\binom{m}{2}}. \quad (5)$$

The Mutual Information [MI] The mutual information is an information theoretic quantity which provides a measure of the dependence between two random variables. In clustering, the mutual information between two partitions quantifies how much information about one cluster membership is revealed by knowing the other partition. The mutual information between partitions \mathbf{U} , \mathbf{V} of \mathbf{X}' is

$$\text{MI}(\mathbf{U}, \mathbf{V}) = \sum_{i=1}^{k_1} \sum_{j=1}^{k_2} \frac{|U_i \cap V_j|}{m} \log \left(\frac{\frac{|U_i \cap V_j|}{m}}{\frac{|U_i| \times |V_j|}{m^2}} \right). \quad (6)$$

Given clustering functions $\psi(\cdot; \mathbf{X})$ and $\psi(\cdot; \mathbf{X}')$, we use the Rand index $\text{RI}(\Psi(\mathbf{X}'; \mathbf{X}), \Psi(\mathbf{X}'; \mathbf{X}'))$, or the mutual information $\text{MI}(\Psi(\mathbf{X}'; \mathbf{X}), \Psi(\mathbf{X}'; \mathbf{X}'))$ as replicability metric of the clustering learned on \mathbf{X} and tested on \mathbf{X}' .

Adjustments to Improve Interpretability A desirable property that should be shared across replicability metrics is that they should yield, at least in expectation, a constant and common baseline value when applied to independent random partitions. That is to say, if we repeatedly create independent random partitions \mathbf{U} and \mathbf{V} of \mathbf{X}' , then on average the replicability measure chosen should be a baseline, constant value. This is generally not the case for either the Rand index or the mutual information. To overcome this shortcoming, we adopt the standard solution of Hubert and Arabie [1985], and derive “adjusted” indices satisfying the property above when applied to independent random clusterings. First, we fix a probabilistic model according to which random partitions are generated. We follow the standard convention and choose the permutation model [Lancaster and Seneta, 1969], in which clusterings are generated at random under the constraint of a fixed number of clusters, and a fixed number of points within each cluster. Under this model, we define the following adjusted metric:

$$r^*(\mathbf{U}, \mathbf{V}) = \frac{r(\mathbf{U}, \mathbf{V}) - \mathbb{E}_{\tilde{\mathbf{U}}, \tilde{\mathbf{V}}}[r(\tilde{\mathbf{U}}, \tilde{\mathbf{V}})]}{\max_{\mathbf{U}', \mathbf{V}'} \{r(\mathbf{U}', \mathbf{V}')\} - \mathbb{E}_{\tilde{\mathbf{U}}, \tilde{\mathbf{V}}}[r(\tilde{\mathbf{U}}, \tilde{\mathbf{V}})]},$$

where $r(\mathbf{U}, \mathbf{V})$ denotes the unadjusted replicability metric (RI or MI) between partitions \mathbf{U} and \mathbf{V} of the same dataset \mathbf{X}' . Given \mathbf{U} and \mathbf{V} and their subsets' sizes, the terms $\mathbb{E}_{\tilde{\mathbf{U}}, \tilde{\mathbf{V}}}[r(\tilde{\mathbf{U}}, \tilde{\mathbf{V}})]$ and $\max_{\mathbf{U}', \mathbf{V}'}\{\mathbf{U}', \mathbf{V}'\}$ appearing in the denominator of the equation above are obtained by respectively integrating and maximizing over the set of partitions with k_1 and k_2 subsets having sizes $\{|U_k|\}_{k=1}^{k_1}$ and $\{|V_j|\}_{j=1}^{k_2}$ with respect to the permutation model of Lancaster and Seneta [1969]. We henceforth adopt the adjusted replicability indices described above: the adjusted Rand index (ARI) and mutual information (AMI), and replace them in Equations (5) and (6). For additional details on this approach, see Vinh et al. [2009, 2010].

3.3 Quantifying Cross-Study Replicability of Cluster Analyses

3.3.1 Replicability on a Single Testing Dataset

Let \mathbf{X}, \mathbf{X}' be independent datasets consisting of n and m data points respectively. To capture heterogeneity caused by different measurement technologies, errors in the measurement processes, and other factors, we model each dataset as a collection of independent and identically distributed draws from separate distributions F_1 and F_2 with support on \mathbb{R}^p . Our goal is to evaluate the replicability of clustering algorithm \mathcal{A} trained on data \mathbf{X} drawn from F_1 and validated on data \mathbf{X}' from F_2 . To capture it, we define the cross-study cluster analysis replicability index

$$R(F_2; \mathcal{A}, F_1) = \mathbb{E}[r^*(\Psi(\mathbf{Z}'; \mathcal{A}, \mathbf{Z}), \Psi(\mathbf{Z}'; \mathcal{A}, \mathbf{Z}'))], \quad (7)$$

where $\mathbf{Z} = \{Z_1, \dots, Z_n\}$ is a collection of n i.i.d. random replicates from F_1 , and $\mathbf{Z}' = \{Z'_1, \dots, Z'_m\}$ is a collection of m i.i.d. random replicates from F_2 . We refer to the index in Equation (7) as R .

Notice that this index depends implicitly also on the sample sizes n, m of the training and testing datasets. Indeed, useful replicability metrics will typically depend on sample size, as we discuss in Masoero et al. [2022b, Appendix A.3]. A point estimate of R is obtained via $\hat{R} := r^*(\Psi(\mathbf{X}'; \mathcal{A}, \mathbf{X}), \Psi(\mathbf{X}'; \mathcal{A}, \mathbf{X}'))$.

To produce interval estimates of R , we employ a bootstrap approach, similar to those proposed for within-study performance (see, e.g. Fang and Wang [2012]). We fix a number B_1 of bootstrap replicates and for each $b \in [B_1]$, we generate bootstrap datasets $\mathbf{X}^{(b)}, \mathbf{X}'^{(b)}$ by sampling with replacement n and m data points from \mathbf{X} and \mathbf{X}' respectively. For every $b \in [B_1]$, we estimate the replicability score $\hat{R}^{(b)} := r^*(\Psi(\mathbf{X}'^{(b)}; \mathcal{A}, \mathbf{X}^{(b)}), \Psi(\mathbf{X}'^{(b)}; \mathcal{A}, \mathbf{X}'^{(b)}))$. The values $\{\hat{R}^{(1)}, \dots, \hat{R}^{(B_1)}\}$ yield an estimate the variability of \hat{R} . We discuss calibration of these estimates in Masoero et al. [2022b, Appendix A.1], and summarize our procedure in Algorithm 1.

3.3.2 Replicability Across a Collection of Datasets

We next consider the scenario in which a collection $\mathcal{X} = \{\mathbf{X}_1, \dots, \mathbf{X}_S\}$ of $S > 2$ datasets is available. Each \mathbf{X}_s contains n_s samples of the same p features.

Extending the ideas of Section 3.3.1, we define the cross-study replicability of algorithm \mathcal{A} trained on dataset \mathbf{X}_1 and tested on $\mathbf{X}_{s'}$, $s' = 2, \dots, S$ as the average over pairwise replicability scores:

$$\mathcal{R}(\{F_{s'}\}_{s'=2,\dots,S}; \mathcal{A}, F_1) = \sum_{s' \neq 1} \frac{R(F_{s'}; \mathcal{A}, F_1)}{S-1}, \quad (8)$$

with $R(F_{s'}; \mathcal{A}, F_s)$ defined in Equation (7). Similiar expressions can be defined for training sets other than \mathbf{X}_1 . A point estimate $\hat{\mathcal{R}}$ of $\mathcal{R}(\{F_{s'}\}_{s'=2,\dots,S}; \mathcal{A}, F_1)$ is obtained by replacing each score $R(F_{s'}; \mathcal{A}, F_1)$ with its sample counterpart $\hat{R}_{s'} := r^*(\Psi(\mathbf{X}_{s'}; \mathcal{A}, \mathbf{X}_1), \Psi(\mathbf{X}_{s'}; \mathcal{A}, \mathbf{X}_{s'}))$. We adopt the same approach as before to produce interval estimates of \mathcal{R} . Fix a number B_2 of iterations, and for each $b \in [B_2]$ draw a bootstrap copy $\mathbf{X}_s^{(b)}$ from \mathbf{X}_s , $s \in [S]$. We learn clustering functions $\psi(\cdot; \mathcal{A}, \mathbf{X}_s^{(b)})$, $s \in [S]$, and compute for each $s' = 2, \dots, S$ the replicability index $\hat{R}_{s'}^{(b)} := r^*(\Psi(\mathbf{X}_{s'}^{(b)}; \mathcal{A}, \mathbf{X}_1^{(b)}), \Psi(\mathbf{X}_{s'}^{(b)}; \mathcal{A}, \mathbf{X}_{s'}^{(b)}))$. Then, for every $b \in [B_2]$, compute $\hat{\mathcal{R}}^{(b)} := (\hat{R}_2^{(b)} + \dots + \hat{R}_S^{(b)}) / (S-1)$. The values $\{\hat{\mathcal{R}}_1^{(1)}, \dots, \hat{\mathcal{R}}_1^{(B_2)}\}$ are used to produce intervals around $\hat{\mathcal{R}}(\{\mathbf{X}_{s'}\}_{s'=2,\dots,S}; \mathcal{A}, \mathbf{X}_1)$, as described in Algorithm 2.

Algorithm 1

- 1: **procedure** Fix clustering algorithm \mathcal{A} , replicability index r , number of bootstrap iterations B_1 . Let \mathbf{X} and \mathbf{X}' be training and testing datasets.
 - 2: **for** $b = 1, \dots, B_1$ **do**
 - 3: Draw bootstrap samples $\mathbf{X}^{(b)}, \mathbf{X}'^{(b)}$ from \mathbf{X}, \mathbf{X}' .
 - 4: Learn $\psi(\cdot; \mathbf{X}^{(b)})$ and $\psi(\cdot; \mathbf{X}'^{(b)})$.
 - 5: Compute $\hat{R}^{(b)} = r^*(\Psi(\mathbf{X}'^{(b)}; \mathbf{X}^{(b)}), \Psi(\mathbf{X}'^{(b)}; \mathbf{X}'^{(b)}))$.
 - 6: **return** $\hat{R}^{(1)}, \dots, \hat{R}^{(B_1)}$.
-

Algorithm 2

- 1: **procedure** Fix clustering algorithm \mathcal{A} , replicability index r , number of bootstrap iterations B_2 , training dataset \mathbf{X}_t , $t \in [S]$. Let $\mathcal{X} = \{X_1, \dots, X_S\}$ be the collection of available datasets.
 - 2: **for** $b = 1, \dots, B_2$ **do**
 - 3: **for** $s = 1, \dots, S$ **do**
 - 4: Draw bootstrap sample $\mathbf{X}_s^{(b)}$ from \mathbf{X}_s .
 - 5: Learn $\psi(\cdot; \mathbf{X}_s^{(b)})$.
 - 6: **for** $s = 1, \dots, S$, $s \neq t$ **do**
 - 7: Let $\hat{R}_s^{(b)} = r^*(\Psi(\mathbf{X}_s^{(b)}; \mathbf{X}_t^{(b)}), \Psi(\mathbf{X}_s^{(b)}; \mathbf{X}_s^{(b)}))$.
 - 8: Let $\hat{\mathcal{R}}^{(b)} = \frac{1}{S-1} \sum_{s \neq t} \hat{R}_s^{(b)}$.
 - 9: **return** $\hat{\mathcal{R}}^{(1)}, \dots, \hat{\mathcal{R}}^{(B_2)}$.
-

3.3.3 Local Replicability: Validating Individual Clusters

The replicability indices produced by Algorithms 1 and 2 provide measures to quantify which clustering procedures are reproducible across multiple datasets at a *global* scale. A natural additional desideratum for a reproducible clustering procedure is that it will induce partitions that are similar also locally. Indeed, sometimes, the clusterings found on two or more datasets can agree on the majority of the sample space, leading to high replicability scores, but disagree on a smaller portion. For example, when two datasets are available, one clustering might completely miss a small cluster that is clearly identified by the other. The replicability scores provided by Algorithms 1 and 2 can fail to capture this pattern. Conversely, it may be that the two clusterings disagree almost everywhere, but are able to identify one or a few robust clusters. In this case, the replicability scores might be poor, and fail to provide insight about which clusters are reproduced across datasets. In applications, measuring which clusters replicate across datasets is important, as it can provide insights about the presence or absence of specific groups of practical interest.

As before, let \mathbf{X} , \mathbf{X}' be the training and testing datasets, from distributions F_1 and F_2 respectively. We now present a strategy to leverage the replicability scores when one is interested in understanding local replicability, with respect to a point of interest $x \in \mathbb{R}^p$. For example, x can be a specific patient clinical profile. We can quantify whether clustering algorithm \mathcal{A} produces similar results in the neighborhood of x when trained on data \mathbf{X} and tested on data \mathbf{X}' via the following “local replicability score” (LR):

$$\text{LR}(F_2; \mathcal{A}, F_1, x) = \mathbb{E}[r^*(\tilde{\Psi}_x(\mathbf{Z}'; \mathcal{A}, \mathbf{Z}), \tilde{\Psi}_x(\mathbf{Z}'; \mathcal{A}, \mathbf{Z}'))].$$

Notice that the local replicability score LR is simply obtained by replacing the clustering function ψ used in Equation (7) with the binary clustering operator $\tilde{\psi}_x$. If x belongs to a reproducible cluster, then the two binary partitions should be similar, and the local replicability score high. Conversely, if x is a data point within a cluster with low reproducibility, these binary partitions differ, and local replicability scores will be low. We adopt the same approach used in Algorithms 1 and 2 to obtain bootstrap confidence intervals (see Algorithm 3 for details).

Cluster-Specific Replicability The procedure outlined above quantifies replicability with respect to a single point, but the same strategy can be used to assess replicability at a cluster level. For example, to assess the replicability of cluster $U_1 \subset \mathbf{X}$, we average the local replicability scores with respect to all points $x \in U_1$.

Multiple Studies When multiple studies $\mathbf{X}_1, \dots, \mathbf{X}_S$ are available and we are interested in studying the local replicability of a clustering learned on a training set \mathbf{X}_s when validated against \mathbf{X}_t , $t \neq s$, we can simply perform Algorithm 3 for all pairs of datasets (s, t) , $t = 1, \dots, s - 1, s + 1, \dots, S$.

Algorithm 3

1: **procedure** Fix clustering algorithm, replicability index r , number of bootstrap iterations B_3 , $x \in \mathbb{R}^p$.
2: **for** $b = 1, \dots, B_3$ **do**
3: Draw bootstrap samples $\mathbf{X}^{(b)}$ from \mathbf{X} , $\mathbf{X}'^{(b)}$ from \mathbf{X}' .
4: Learn $\psi(\cdot; \mathbf{X}^{(b)})$ and $\psi(\cdot; \mathbf{X}'^{(b)})$.
5: Let $\widehat{\text{LR}}^{(b)} = r^*(\tilde{\Psi}_x(\mathbf{X}'^{(b)}; \mathbf{X}^{(b)}), \tilde{\Psi}_x(\mathbf{X}'^{(b)}; \mathbf{X}'^{(b)}))$
6: **return** $\widehat{\text{LR}}^{(1)}, \dots, \widehat{\text{LR}}^{(B_3)}$

4 Simulation Study

4.1 Homogeneous Datasets

To demonstrate the usefulness of the replicability metrics introduced, we start by showing, on synthetic data, how the replicability index can guide the choice of the number of clusters and clustering algorithm. We consider four popular clustering algorithms: Birch [Zhang et al., 1996], k -means, mini-batch k -means [Lloyd, 1982], and agglomerative clustering [Ward Jr, 1963]. All these procedures take the number of clusters k as an input. Because we expect to observe high replicability scores when an appropriate algorithm and number of clusters are chosen, we show how the replicability index can be used to (i) tune the number of clusters for each algorithm and (ii) choose which algorithm to use.

In our experiments, we use a collection of benchmark datasets (see the first column of Figure 1) [Fränti and Sieranoja, 2018]. We partition each dataset into training and testing sets of equal size, and for each $k \in \text{range}_{40} = \{2, 3, \dots, 40\}$, we run Algorithm 1 for each clustering algorithm for $B_1 = 100$ bootstrap iterations. Our results are illustrated in Figure 1. We highlight three important features of the cross-study replicability estimates obtained:

- When the clusters are well separated, and the clustering algorithms used are appropriate for the shape of the clusters, the replicability indices achieve the highest scores at the “true” number of clusters (see datasets A and B).
- When the number of clusters is less obvious, as in dataset C , the replicability scores tend to be less peaked around a single value, indicating uncertainty on the number of clusters that should be selected to maximize replicability.
- Sometimes, a clustering structure is present in the data, but algorithms fail to capture it. For example, for dataset D , the only successful algorithm is DBSCAN (Ester et al. [1996], purple line), which achieves good replicability scores for $k = 2, 3$. In this case (D), the replicability index can aid the choice of the most appropriate clustering algorithm for the data at hand.

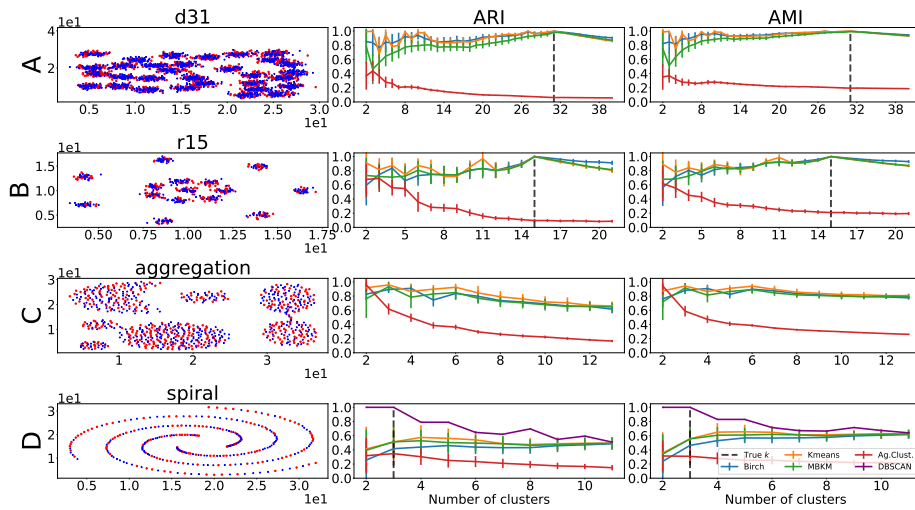


Figure 1: Reproducibility scores produced by Algorithm 1 on benchmark datasets [Fränti and Sieranoja, 2018]. Left column: datasets (*d31* (A), *r15* (B), *aggregation* (C), *spiral* (D)) randomly divided in training (red points) and testing (blue points) datasets of equal size. Center and right columns: replicability scores (vertical axis) using AMI (center) and ARI (right), versus number of clusters k (horizontal axis). We used Algorithm 1 with $B = 100$ bootstrap iterations across different input values k and clustering algorithms. We plot the mean score \pm one standard deviation across bootstrap runs. The number of data points in datasets $A - D$ varies widely (*d31*: $n = 3100$, *r15*: $n = 600$, *aggregation*: $n = 788$, *spiral*: $n = 312$).

4.2 Heterogeneous Datasets

To test Algorithm 2, we consider datasets drawn from high-dimensional Gaussian mixture models. Through heterogeneity of the data generating distributions, we simulate differences we expect to observe across different groups of studies. A datapoint in the s -th study is drawn as follows:

$$x_{s,i} \stackrel{i.i.d.}{\sim} F_{z_s} = \sum_{\ell=1}^k \pi_{\ell}^{(z_s)} \mathcal{N}\left(\mu_{\ell}^{(z_s)}, \Sigma_{\ell}^{(z_s)}\right),$$

for $s = 1, \dots, S$ and $i = 1, \dots, n_s$. Here, z_s is an index identifying the reference distribution from which dataset s is generated, $\pi_{\ell}^{(z_s)} \in (0, 1)$ are mixing proportions such that $\sum_{\ell} \pi_{\ell}^{(z_s)} = 1$, and $\mathcal{N}(\mu_{\ell}^{(z_s)}, \Sigma_{\ell}^{(z_s)})$ denotes a Gaussian distribution with mean $\mu_{\ell}^{(z_s)}$ and covariance matrix $\Sigma_{\ell}^{(z_s)}$. We set $S = 4$ and assume $\mathbf{X}_1, \mathbf{X}_2$ are drawn from the same mixture of Gaussians F_1 (i.e. $z_1 = z_2 = 1$), while $\mathbf{X}_3, \mathbf{X}_4$ are drawn from a second, different mixture of Gaussians F_2 (i.e. $z_3 = z_4 = 2$). Specifically, F_1 and F_2 are mixtures of Gaussians with $k = 16$ components, each component with the same covariance matrix $\Sigma = I$, where I is the identity matrix. The mean vectors of F_1 are denoted by $\mu_{\ell}^{(1)} \in \mathbb{R}^{64}$, $\ell = 1, \dots, 16$, and induce well separated components. The mean vectors of F_2 are denoted by $\mu_{\ell}^{(2)} \in \mathbb{R}^{64}$, $\ell = 1, \dots, 16$ and are obtained as follows: first a permutation $\pi(\cdot) : [32] \rightarrow [32]$ of the first 32 coordinates is chosen, and then each vector $\mu_{\ell}^{(2)}$ is obtained by permuting the first 32 coordinates of $\mu_{\ell}^{(1)}$ according to $\pi(\cdot)$. In this way, both F_1 and F_2 have $k = 16$ well separated - albeit, different - components (see [Fränti et al., 2006] for further description of these distributions).

We compute and report, for every pair \mathbf{X}_s and \mathbf{X}_t of datasets, $s, t = 1, \dots, 4$ the average replicability score (Figure 2) for different clustering methods. As expected, replicability scores are always higher when comparing two datasets drawn from the same distribution, hence sharing the same clustering structure (top left and bottom right block diagonals of each of the 16 sub-panels in Figure 2), while they are substantially lower when comparing datasets from different distributions. We also notice that all the clustering algorithms have better replicability when the correct number of clusters is specified as input, and that *Affinity propagation* [Frey and Dueck, 2007] seems to be performing overall worse than the other algorithms.

4.3 Local Replicability

To illustrate Algorithm 3, we consider $S = 2$ datasets, \mathbf{X}, \mathbf{X}' with 100 datapoints each, drawn from Gaussian mixture models F_1 and F_2 in eq. (9) with three components and support on \mathbb{R}^2 . F_1 and F_2 share two of the three components: letting $\mathcal{N}(\mu, \sigma^2)$ denote the distribution of a Gaussian random variable with mean μ and variance σ^2 ,

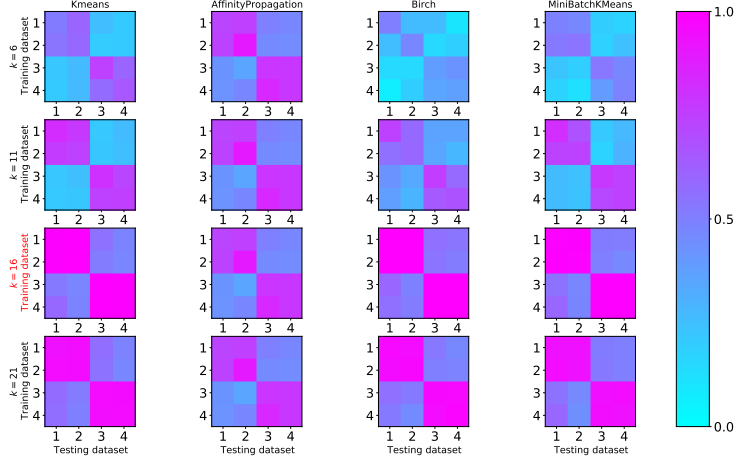


Figure 2: ARI scores for 4 datasets in \mathbb{R}^{64} , $B = 100$ bootstrap runs. Along the rows we vary the number of clusters $k \in \{6, 11, 16, 21\}$, 16 is the true number of clusters. Along the columns we vary the clustering algorithms.

$$\begin{aligned}
 F_1 &= \sum_{j \in \{A, B, C\}} \frac{1}{3} \mathcal{N}(\mu_j, \sigma^2 I), \\
 F_2 &= \sum_{\ell \in \{A, B, D\}} \frac{1}{3} \mathcal{N}(\mu_\ell, \sigma^2 I).
 \end{aligned} \tag{9}$$

We let $\sigma = 0.2$, $\mu_A = [-2, -2]^\top$, $\mu_B = [0, 2]^\top$, $\mu_C = [2, -2]^\top$ and $\mu_D = [-13/10, 13/20]^\top$. We refer to the mixture component identified by μ_A as component A , and similarly for the other components B, C, D . \mathbf{X} has three well separated clusters, while two of the three clusters in \mathbf{X}' are closer to each other (see Figure 4).

The goal here is to quantify, at a fixed data point x , local replicability, as discussed in Section 3.3.3. For example, x could be a point of \mathbf{X}, \mathbf{X}' , or any point in the support of the distribution. In our experiments, Algorithm 3 is able to capture the different replicability properties of individual clusters, providing substantially different scores for points belonging to different clusters.

We illustrate the mechanics of the algorithm, and its ability to capture local replicability in Figure 3: in column (a), we consider a point x_A close to μ_A , which does not belong to the \mathbf{X} and \mathbf{X}' datasets, and is identified by the ∇ symbol. Component A is present both in \mathbf{X} and \mathbf{X}' , and the associated cluster replicates across the two datasets. Indeed, across the $B_3 = 100$ iterations, the two binary partitions $\tilde{\Psi}_{x_A}(\mathbf{X}'^{(b)}, \mathbf{X}^{(b)})$ and $\tilde{\Psi}_{x_A}(\mathbf{X}'^{(b)}, \mathbf{X}'^{(b)})$ (top, bottom row) are similar, and the replicability score relatively high. In column (b), we consider instead a point x_B belonging to the cluster induced by component B , identified

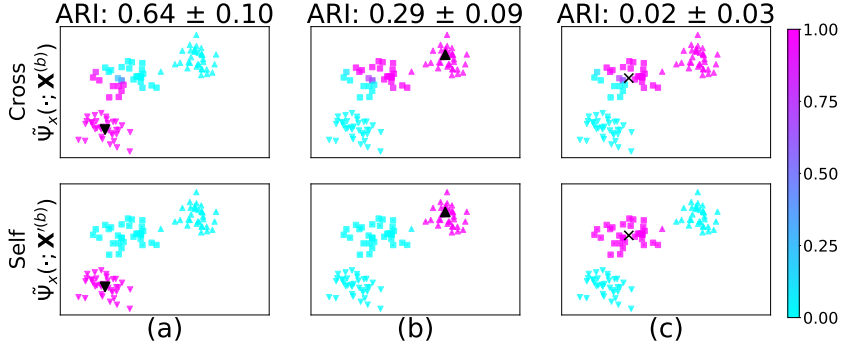


Figure 3: Local replicability with k -means, $k = 3$. Both rows show the test dataset \mathbf{X}' . Column (a): we fix test point x_A from component A (in black). We color each data point $x' \in \mathbf{X}'$ according to the average of $\{\psi_{x_A}(x'; \mathbf{X}^{(b)})\}_{b=1}^{1000}$ (top row), $\{\tilde{\psi}_{x_A}(x'; \mathbf{X}'^{(b)})\}_{b=1}^{1000}$ (bottom row). $\mathbf{X}^{(b)}, \mathbf{X}'^{(b)}$ are bootstrap draws from \mathbf{X}, \mathbf{X}' . We compute the LR (ARI) $\{r^*(\tilde{\Psi}_{x_A}(\mathbf{X}'^{(b)}; \mathbf{X}^{(b)}), \tilde{\Psi}_{x_A}(\mathbf{X}'^{(b)}; \mathbf{X}'^{(b)}))\}_{b=1}^{1000}$, and report the average score \pm one standard deviation on top of column (a). This is high whenever the color pattern in the two rows is similar. Columns (b) and (c) replicate the analysis using points x_B and x_C from components B and C .

by the \triangle symbol. In \mathbf{X} , this cluster is well separated from the clusters induced by the other components. However, in \mathbf{X}' , the cluster induced by component B is close to the cluster induced by the component D , whose data points are identified with the \square symbol, affecting the replicability score associated with x_B . The binary partitions $\tilde{\Psi}_{x_B}(\mathbf{X}'; \mathbf{X})$ and $\tilde{\Psi}_{x_B}(\mathbf{X}'; \mathbf{X}')$ are different. $\tilde{\Psi}_{x_B}(\mathbf{X}'; \mathbf{X})$ incorrectly indicates points from the components B and D as belonging to the same cluster, while the partition $\tilde{\Psi}_{x_B}(\mathbf{X}'; \mathbf{X}')$ does not incur into this problem. This discrepancy negatively affects the local replicability score. Last, in column (c), we consider a point x_C that belongs to the cluster component C in \mathbf{X} (\times symbol). In this case, the scores are essentially equal to 0, since this cluster is absent in \mathbf{X}' . For the same data, we report results for the local replicability test scores at the cluster levels in Figure 4.

5 Breast Cancer Gene Expression Datasets

In this section, we apply our clustering replicability metrics to publicly available breast cancer gene expression datasets that were collected to identify tumor subtypes. We consider the Mainz, Transbig and Vdx datasets [Schroeder et al., 2011a,b,c]. These datasets have been processed and come in the form of a matrix, $\mathbf{X} \in \mathbb{R}^{n \times p}$, where n is the number of samples and p is the number of gene expression measurements. We work with the $p = 22,283$ genes shared by all datasets. The sample sizes vary (Mainz, $n_s = 200$, Transbig, $n_s = 198$, Vdx,

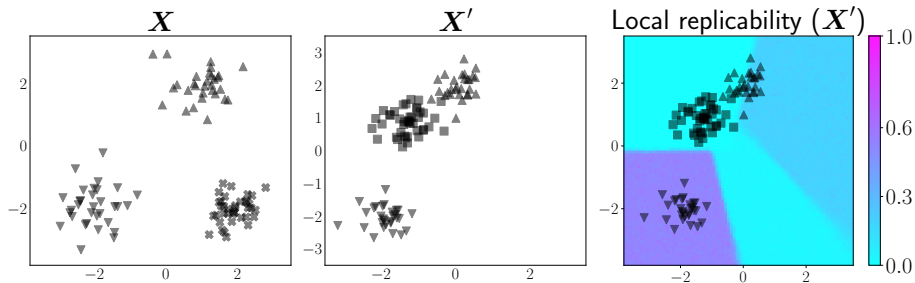


Figure 4: Local replicability. Left: training dataset \mathbf{X} (from F_1). Center: testing dataset \mathbf{X}' (from F_2 , Equation (9)). Different markers identify different components (∇ : A , \triangle : B , \times : C , \square : D). Right: local replicability on \mathbf{X}' . We plot points in \mathbf{X}' , and color the sample space according to the local replicability scores of the partition learned on \mathbf{X} when tested on \mathbf{X}' . Scores (ARI) are obtained by averaging $B_3 = 100$ bootstrap runs over a grid of 250×250 equally spaced points.

$n_s = 344$).

Breast tumors can be classified into subtypes characterized by distinct molecular markers and clinical characteristics. There are four established molecular subtypes of breast cancer. Luminal A tumors are less aggressive than the other subtypes, have lower proliferation, express hormone receptors Estrogen Receptor (ER) and Progesteron Receptor (PR) and do not express the ERBB2 gene. These tumors are sensitive to endocrine therapy and have better prognosis compared to the other subtypes. Luminal B tumors are ER and PR positive, have higher proliferation and may or may not have ERBB2 expression. These tumors are less responsive to hormonal therapy and are more aggressive. The Her2+ subtype is characterized by increased expression of ERBB2 and low levels of ER and PR expression. This tumor subtype is aggressive and patients do not respond to endocrine therapy. Treatment options include ERBB2-targeted therapies. Basal-like breast cancer subtype is characterized by low levels of ER, PR and ERBB2 expression. This is the most aggressive subtype with first and later therapy lines often limited to single-agent chemotherapy [Waks and Winer, 2019]. These subtypes were first identified by applying unsupervised hierarchical clustering to gene expression data from breast tumor tissues [Perou et al., 2000]. In our experiments, for the purpose of comparisons, we take advantage of previously proposed subsets of genes: the PAM50 subset [Parker et al., 2009], which contains fifty genes, and the three genes [3G] subset proposed by Haibe-Kains et al. [2012].

5.1 Global replicability scores

First, we compare the replicability scores of simple clustering methods using Algorithm 1 on the three datasets considered. We use in turn each pair of datasets as training and testing, and analyze how the replicability properties

change as we vary (i) the replicability metric, (ii) the training/testing pair, (iii) the clustering algorithm and the number of clusters k , and (iv) the genes subsets (Figure 5). Four main observations emerge:

- The relative ranking of clustering methods with respect to replicability scores is robust to the choice of ARI or AMI.
- Replicability scores are generally comparable across most pairs of training and testing datasets and produce similar results when the roles of \mathbf{X} and \mathbf{X}' are reversed.
- The choices of clustering algorithm and k play a crucial role in determining replicability scores.
- When using the 3G subset, $k = 3$ yields the highest replicability scores, while with the PAM 50 subset $k = 4$ achieves the highest scores.

Our replicability metric provides consistent results with the subtypes published in Parker et al. [2009] and Haibe-Kains et al. [2012] (see Figure 9 in Masoero et al. [2022b]). Namely, clustering functions achieving high replicability scores produce partitions similar to the classification-based subtypes. This provides evidence that reproducible partitions are also consistent with well accepted biological findings.

5.2 Local replicability scores

Next, we perform a local replicability analysis using Algorithm 3 on the three datasets considered, using both the 3G and PAM50 gene subsets. We find that the cluster associated with the Basal subtype is the easiest to identify and the most robust, with the highest local replicability score. Luminal A and Luminal B are harder to distinguish, and are associated with lower local replicability scores.

In Figure 6 we provide a visualization of our findings. We use the 3G subset, the Transbig (\mathbf{X}') dataset [Schroeder et al., 2011b] for testing, and the Mainz (\mathbf{X}) dataset [Schroeder et al., 2011a] for training. To produce Figure 6, for each point $x \in \mathbf{X}'$ we compute the local replicability score using Algorithm 3, using k -means with $k = 4$, \mathbf{X} as training set and $B = 100$ bootstrap iterations. To group datapoints in \mathbf{X}' into different clusters, we use $\Psi(\mathbf{X}'; \mathbf{X})$. The partition obtained closely resembles the model-based signature $\Pi_{3G}(\mathbf{X}')$ provided by Haibe-Kains et al. [2012]. We therefore match each learned cluster to one of the cancer subtypes labels, so that each cluster corresponded to one cancer subtype (Luminal A, Luminal B, Basal, Her2+). The average local replicability scores within each block of the partition confirm what expected: the Basal subtype is the most reproducible, while Luminal A and Luminal B are the least reproducible.

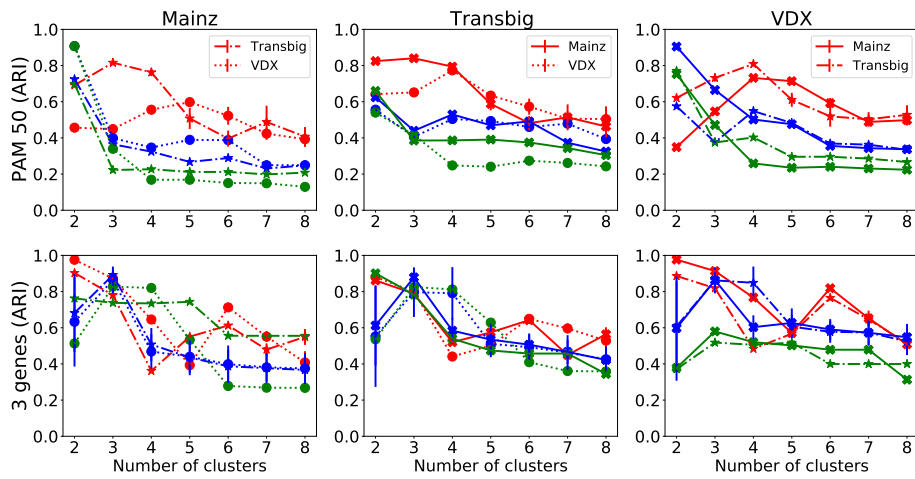


Figure 5: Average replicability scores using Algorithm 1 on cancer datasets of Schroeder et al. [2011a,b,c]. Each row identifies a gene subset (top: PAM50 [Parker et al., 2009], bottom: 3G [Haibe-Kains et al., 2012]). Each column identifies a testing datasets (from left to right: Schroeder et al. [2011a,b,c]). For each pair of gene subset and test dataset, we separately consider each of the remaining two datasets as the training set. Line styles identify the training set used. We use k -means (red), Birch (green), and agglomerative clustering (blue), for $k \in \{2, 3, \dots, 8\}$, and report the average replicability scores (ARI) across $B = 100$ iterations \pm one standard deviation (vertical axis).

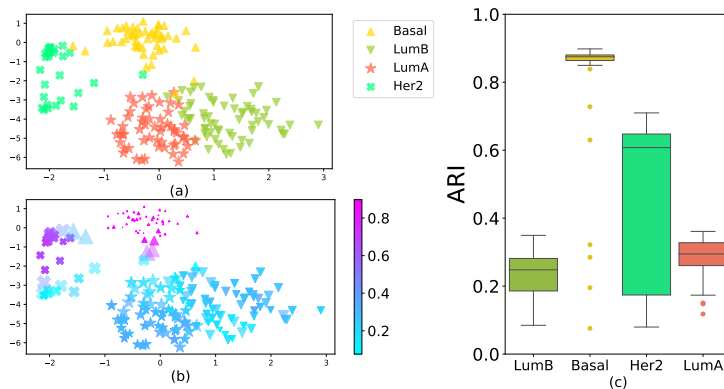


Figure 6: Local replicability of observed points in Transbig (\mathbf{X}' , Schroeder et al. [2011b]) when Mainz (\mathbf{X} , Schroeder et al. [2011a]) is used for training. We use the 3G subset [Haibe-Kains et al., 2012] and k -means, $k = 4$. In (a), we visualize \mathbf{X}' . Points are grouped into different clusters according to $\Psi(\mathbf{X}'; \mathbf{X})$, which closely resembles $\Pi_{3G}(\mathbf{X}')$, so we can assign one cancer subtype to each cluster. In (b), we report the local replicability scores obtained by running Algorithm 3 on every point $x' \in \mathbf{X}'$. Colors reflects the average local replicability (AMI) score, while the size and transparency are proportional to the standard deviation across the bootstrap iterations: larger points have more variable scores. We plot the data using a tSNE embedding with well separated clusters [Maaten and Hinton, 2008]. In (c), for each cluster subtype (as defined by $\Psi(\mathbf{X}'; \mathbf{X})$), we report ARI scores.

6 Discussion

In this paper, we provide a cohesive review of existing methods for replicability of clustering analyses, and develop a novel framework for replicability of clustering when multiple datasets are available. This new approach allows to quantify replicability with any number of datasets and using any clustering algorithm, at a local as well as at a global scale. In our experiments, we show that our replicability scores guide the choice of an effective clustering algorithm and the tuning of relevant parameters, such as the number of clusters used in the analysis. Our evaluation procedures build on the bootstrap method: using bootstrap subsamples allows to quantify uncertainty summaries and interval estimates, making the replicability scores more informative (see Masoero et al. [2022b, Appendix A.1]). The bootstrap approach mitigates the impact of outliers on the replicability scores. We report additional experiments in Masoero et al. [2022b, Appendices A, C]: these are conducted using our method, as well as the methods reviewed in Section 2. Our experimental findings suggest that our method is a valuable tool for replicability analyses. In applications, our newly proposed metrics can help choosing which clustering algorithm to use, suggesting which method is best for the analysis of the data at hand. Last, while we have here focused on clustering algorithms, we emphasize that there exists a large literature on random partition models and statistical modeling that can be useful for clustering problems (see, e.g. Müller and Quintana [2010], Wade and Ghahramani [2018]).

Acknowledgments LT has been supported by the NIH grant 5R01LM013352-02 and the NSF grant 2113707.

References

- A. N. Albatineh, M. Niewiadomska-Bugaj, and D. Mihalko. On similarity indices and correction for chance agreement. *Journal of Classification*, 23(2), 2006.
- G. Alexe, G. S. Dalgin, R. Ramaswamy, C. DeLisi, and G. Bhanot. Data perturbation independent diagnosis and validation of breast cancer subtypes using clustering and patterns. *Cancer Informatics*, 2, 2006.
- A. B. Arrieta, N. Díaz-Rodríguez, J. Del Ser, A. Bennetot, S. Tabik, A. Barbado, S. García, S. Gil-López, D. Molina, and R. Benjamins. Explainable artificial intelligence (xai): Concepts, taxonomies, opportunities and challenges toward responsible ai. *Information fusion*, 58:82–115, 2020.
- S. Ben-David, D. Pál, and H. U. Simon. Stability of k -means clustering. In *International Conference on Computational Learning Theory*. Springer, 2007.
- C. Bernau, M. Riester, A.-L. Boulesteix, G. Parmigiani, C. Huttenhower, L. Waldron, and L. Trippa. Cross-study validation for the assessment of prediction algorithms. *Bioinformatics*, 30(12), 2014.

- A. Bertoni and G. Valentini. Model order selection for bio-molecular data clustering. *BMC Bioinformatics*, 8(2), 2007.
- G. Brock, V. Pihur, S. Datta, and S. Datta. clvalid: An R package for cluster validation. *Journal of Statistical Software*, 25, 2008.
- J. Bryan. Problems in gene clustering based on gene expression data. *Journal of Multivariate Analysis*, 90(1), 2004.
- M. Ester, H.-P. Kriegel, J. Sander, and X. Xu. A density-based algorithm for discovering clusters in large spatial databases with noise. *Proceedings of the Second International Conference on Knowledge Discovery and Data Mining*, 1996.
- Y. Fang and J. Wang. Selection of the number of clusters via the bootstrap method. *Computational Statistics & Data Analysis*, 56(3), 2012.
- P. Fränti and S. Sieranoja. K-means properties on six clustering benchmark datasets. *Applied Intelligence*, 48(12), 2018.
- P. Fränti, O. Virmajoki, and V. Hautamäki. Fast agglomerative clustering using a k -nearest neighbor graph. *IEEE Transactions on Pattern Analysis and Machine Intelligence*, 28(11), 2006.
- B. J. Frey and D. Dueck. Clustering by passing messages between data points. *Science*, 315(5814), 2007.
- B. Haibe-Kains, C. Desmedt, S. Loi, A. C. Culhane, G. Bontempi, J. Quackenbush, and C. Sotiriou. A three-gene model to robustly identify breast cancer molecular subtypes. *Journal of the National Cancer Institute*, 104(4), 2012.
- D. N. Hayes, S. Monti, G. Parmigiani, C. B. Gilks, K. Naoki, A. Bhattacharjee, M. A. Socinski, C. Perou, and M. Meyerson. Gene expression profiling reveals reproducible human lung adenocarcinoma subtypes in multiple independent patient cohorts. *Journal of Clinical Oncology*, 24(31), 2006.
- C. Hennig. Cluster-wise assessment of cluster stability. *Computational Statistics & Data Analysis*, 52(1), 2007.
- C. Hennig. Package ‘fpc’. *R-project*, 91, 2015.
- L. Hubert and P. Arabie. Comparing partitions. *Journal of Classification*, 2(1), 1985.
- P. A. Jaskowiak, R. J. Campello, and I. G. Costa. On the selection of appropriate distances for gene expression data clustering. *BMC Bioinformatics*, 15(2):S2, 2014.
- A. V. Kapp and R. Tibshirani. Are clusters found in one dataset present in another dataset? *Biostatistics*, 8(1), 2006.

- H. O. Lancaster and E. Seneta. Chi-square distribution. *Encyclopedia of Biostatistics*, 2, 1969.
- T. Lange, V. Roth, M. L. Braun, and J. M. Buhmann. Stability-based validation of clustering solutions. *Neural Computation*, 16(6), 2004.
- M. A. Levenstien, Y. Yang, and J. Ott. Statistical significance for hierarchical clustering in genetic association and microarray expression studies. *BMC Bioinformatics*, 4(1), 2003.
- E. Levine and E. Domany. Resampling method for unsupervised estimation of cluster validity. *Neural Computation*, 13(11), 2001.
- C. Lim and B. Yu. Estimation stability with cross-validation (escv). *Journal of Computational and Graphical Statistics*, 25(2):464–492, 2016.
- Y. Liu, D. N. Hayes, A. Nobel, and J. S. Marron. Statistical significance of clustering for high-dimension, low-sample size data. *Journal of the American Statistical Association*, 103(483), 2008.
- S. Lloyd. Least squares quantization in PCM. *IEEE Transactions on Information Theory*, 28(2), 1982.
- L. v. d. Maaten and G. Hinton. Visualizing data using t-SNE. *Journal of Machine Learning Research*, 9(Nov), 2008.
- L. Masoero, E. Thomas, G. Parmigiani, S. Tyekucheva, and L. Trippa. Cross-study replicability in cluster analysis. *Statistical Science*, 2022a.
- L. Masoero, E. Thomas, G. Parmigiani, S. Tyekucheva, and L. Trippa. Supplementary material for “cross-study replicability in cluster analysis”. *Statistical Science*, 2022b.
- L. M. McShane, M. D. Radmacher, B. Freidlin, R. Yu, M.-C. Li, and R. Simon. Methods for assessing reproducibility of clustering patterns observed in analyses of microarray data. *Bioinformatics*, 18(11), 2002.
- P. Müller and F. Quintana. Random partition models with regression on covariates. *Journal of Statistical Planning and Inference*, 140(10):2801–2808, 2010.
- W. J. Murdoch, C. Singh, K. Kumbier, R. Abbasi-Asl, and B. Yu. Definitions, methods, and applications in interpretable machine learning. *Proceedings of the National Academy of Sciences*, 116(44):22071–22080, 2019.
- E. National Academies of Sciences and Medicine. *Reproducibility and Replicability in Science*. The National Academies Press, Washington, DC, 2019.

- J. S. Parker, M. Mullins, M. C. Cheang, S. Leung, D. Voduc, T. Vickery, S. Davies, C. Fauron, X. He, Z. Hu, J. F. Quackenbush, I. J. Stijleman, J. Palazzo, J. Marron, A. B. Nobel, E. Mardis, T. O. Nielsen, M. J. Ellis, C. M. Perou, and P. S. Bernard. Supervised risk predictor of breast cancer based on intrinsic subtypes. *Journal of Clinical Oncology*, 27(8), 2009.
- C. M. Perou, T. Sørlie, M. B. Eisen, M. Van De Rijn, S. S. Jeffrey, C. A. Rees, J. R. Pollack, D. T. Ross, H. Johnsen, and L. A. Akslen. Molecular portraits of human breast tumours. *Nature*, 406(6797), 2000.
- W. M. Rand. Objective criteria for the evaluation of clustering methods. *Journal of the American Statistical Association*, 66(336), 1971.
- M. Schroeder, B. Haibe-Kains, A. Culhane, C. Sotiriou, G. Bontempi, and J. Quackenbush. *breastCancerMAINZ: Gene expression dataset published by Schmidt et al. [2008] (MAINZ)*., 2011a. R package version 1.16.0.
- M. Schroeder, B. Haibe-Kains, A. Culhane, C. Sotiriou, G. Bontempi, and J. Quackenbush. *breastCancerTRANSBIG: Gene expression dataset published by Desmedt et al. [2007] (TRANSBIG)*., 2011b. R package version 1.16.0.
- M. Schroeder, B. Haibe-Kains, A. Culhane, C. Sotiriou, G. Bontempi, and J. Quackenbush. *breastCancerVDX: Gene expression datasets published by Wang et al. [2005] and Minn et al. [2007] (VDX)*, 2011c. R package version 1.16.0.
- M. Smolkin and D. Ghosh. Cluster stability scores for microarray data in cancer studies. *BMC Bioinformatics*, 4(1), 2003.
- R. Tibshirani and G. Walther. Cluster validation by prediction strength. *Journal of Computational and Graphical Statistics*, 14(3), 2005.
- L. Trippa, L. Waldron, C. Huttenhower, and G. Parmigiani. Bayesian nonparametric cross-study validation of prediction methods. *The Annals of Applied Statistics*, 9(1), 2015.
- N. X. Vinh, J. Epps, and J. Bailey. Information theoretic measures for clusterings comparison: is a correction for chance necessary? In *Proceedings of the 26th Annual International Conference on Machine Learning*. ACM, 2009.
- N. X. Vinh, J. Epps, and J. Bailey. Information theoretic measures for clusterings comparison: Variants, properties, normalization and correction for chance. *Journal of Machine Learning Research*, 11(Oct), 2010.
- U. Von Luxburg. Clustering stability: an overview. *Foundations and Trends in Machine Learning*, 2(3), 2010.
- S. Wade and Z. Ghahramani. Bayesian cluster analysis: Point estimation and credible balls (with discussion). *Bayesian Analysis*, 13(2):559–626, 2018.

- A. G. Waks and E. P. Winer. Breast cancer treatment: A review. *JAMA*, 321(3), 2019.
- J. H. Ward Jr. Hierarchical grouping to optimize an objective function. *Journal of the American Statistical Association*, 58(301), 1963.
- B. Yu. Stability. *Bernoulli*, 19(4), 2013.
- T. Zhang, R. Ramakrishnan, and M. Livny. Birch: an efficient data clustering method for very large databases. In *ACM Sigmod Record*. ACM, 1996.

A Additional experiments on synthetic data

A.1 Calibration checks for the bootstrap intervals: experimental setup

To assess the usefulness of the bootstrap intervals that are obtained as a byproduct of the output of Algorithm 1 in the main text [Masoero et al., 2022a], we here present a procedure to measure the calibration of these intervals. For this purpose, let F_1 and F_2 be two fixed probability distributions with support on \mathbb{R}^p . Let \mathcal{A} be a fixed clustering algorithm.

Draw n i.i.d. random replicates x_1, \dots, x_n from F_1 , and let $\mathbf{X} = [x_1, \dots, x_n]^\top \in \mathbb{R}^{n \times p}$ be the training set. Similarly, draw m i.i.d. random replicates x'_1, \dots, x'_m from F_2 , and let $\mathbf{X}' = [x'_1, \dots, x'_m]^\top \in \mathbb{R}^{m \times p}$ be the testing dataset. Run Algorithm 1, as detailed in the main text [Masoero et al., 2022a], over a large number B of bootstrap draws from \mathbf{X} and \mathbf{X}' respectively. Given the output $\hat{R}^{(1)}, \dots, \hat{R}^{(B)}$, and for a fixed $\alpha \in [0, 1]$, let $\hat{R}_{(\alpha)}$ be the $100 \times \alpha\%$ quantile of the bootstrap scores $\hat{R}^{(1)}, \dots, \hat{R}^{(B)}$.

To assess the quality of the bootstrap intervals obtained from $\hat{R}_{(\alpha)}$, we compare them to corresponding Monte Carlo values, obtained by repeatedly drawing from F_1 and F_2 . In detail, fix a large N_{MC} . For each $s = 1, \dots, N_{MC}$, draw n i.i.d. random replicates $z_1^{(s)}, \dots, z_n^{(s)}$ from F_1 , and m i.i.d. random replicates $w_1^{(s)}, \dots, w_m^{(s)}$ from F_2 ; let $\mathbf{Z}^{(s)} = [z_1^{(s)}, \dots, z_n^{(s)}]^\top$ and $\mathbf{Z}'^{(s)} = [w_1^{(s)}, \dots, w_m^{(s)}]^\top$. Compute the replicability score $\hat{R}^{(s)} := r^*(\Psi(\mathbf{Z}'^{(s)}; \mathcal{A}, \mathbf{Z}^{(s)}), \Psi(\mathbf{Z}'^{(s)}; \mathcal{A}, \mathbf{Z}^{(s)}))$. Given the output $\hat{R}^{(1)}, \dots, \hat{R}^{(N_{MC})}$, and for a fixed $\alpha \in [0, 1]$, let $\hat{R}_{(\alpha)}$ be the $100 \times \alpha\%$ quantile of the Monte Carlo scores $\hat{R}^{(1)}, \dots, \hat{R}^{(N_{MC})}$. We provide a visual diagnostic, in which we compare the extent to which the Monte Carlo and Bootstrap intervals are similar or differ.

Experimental details

We present experimental results for the setup described above. Here, we let $n = m = 500$, $p = 2$, $B = 1000$, and $N_{MC} = 1000$. The algorithm \mathcal{A} is k -means. We also let F_1, F_2 be mixtures of Gaussians, of the form:

$$F_1 = \frac{1}{4} \sum_{j=1}^4 \mathcal{N}(\mu_j, \sigma I), \quad F_2 = \frac{1}{4} \sum_{j=1}^4 \mathcal{N}(\mu'_j, \sigma I),$$

with $\sigma = 1$, and $\mu_1 = [0, -7], \mu_2 = [3.5, 3], \mu_3 = [-2, 2], \mu_4 = [2, -2]$ and $\mu'_1 = [-1, -7], \mu'_2 = [4.2, 3.3], \mu'_3 = [-2.5, 1.8], \mu'_4 = [2.2, -3]$.

We compare the average replicability score over the Monte Carlo and the bootstrap replicates, together with a centered 95% interval, as we vary the choice k of the number of clusters in Figure 7. We find that, across k , the bootstrap and

Monte Carlo values are very close, showing that the bootstrap intervals enjoy good calibration.

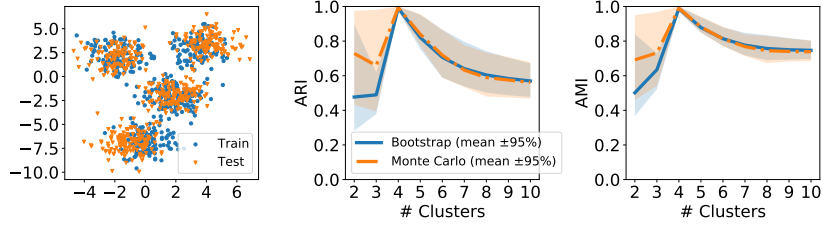


Figure 7: Left: draws $\mathbf{X} \in \mathbb{R}^{500,2}$ (blue), $\mathbf{X}' \in \mathbb{R}^{500,2}$ (orange) from train and test distributions F_1 and F_2 respectively. Center: ARI replicability score when using k -means (vertical axis) for different choices of k (horizontal axis). The blue line reports the average score over $B = 1000$ bootstrap replicates for the two datasets plotted in the left subplot. The orange dotted line reports the average score over $N_{MC} = 1000$ Monte Carlo draws of different pairs of training and testing datasets, drawn the same distributions F_1, F_2 above. Shadowed regions cover a centered 95% interval for the two scores.

Next, we inspect in Figure 8 the calibration of the bootstrap quantiles with respect to the Monte Carlo quantiles. That is, for each α in $[0, 1]$, we compare the values $\hat{R}_{(\alpha)}$ and $\hat{\hat{R}}_{(\alpha)}$. We perform this comparison across different values of k , and verify that the bootstrap and Monte Carlo quantiles are close.

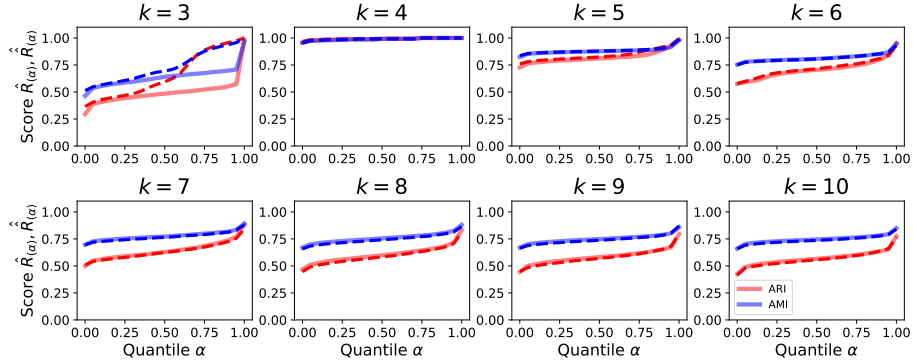


Figure 8: Quantiles coverage. For the same distributions F_1, F_2 considered in Figure 7, each subplot reports the bootstrap (solid lines, $\hat{R}_{(\alpha)}$) and Monte Carlo (dotted lines, $\hat{\hat{R}}_{(\alpha)}$) score (vertical axis) obtained as we increase the quantile (horizontal axis). Red lines refer to ARI, blue lines to AMI.

We repeat the same experiments, for different choices of F_1 and F_2 , as defined

below:

$$F_1 = \frac{1}{4} \sum_{j=1}^4 \mathcal{N}(\mu_j, \sigma I), \quad F_2 = \frac{1}{4} \sum_{j=1}^4 \mathcal{N}(\mu'_j, \sigma I), \quad (10)$$

now with $\mu_1 = [0, -7], \mu_2 = [3.5, -2], \mu_3 = [2, -2]$, and $\mu'_1 = [-1, -7], \mu'_2 = [4.2, -1.8], \mu'_3 = [-2.5, 1.8]$. Plots are included in Figures 9 and 10.

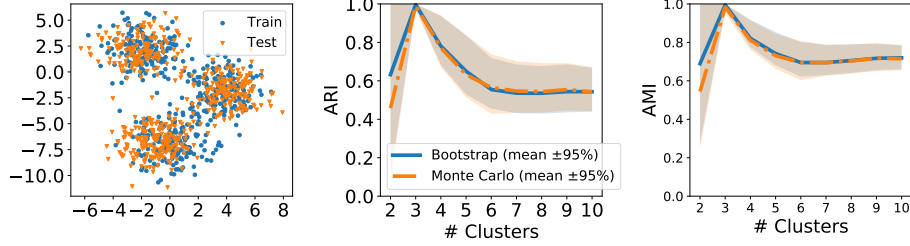


Figure 9: We use the same setup as Figure 7, now for data drawn from the distributions in Equation (10).

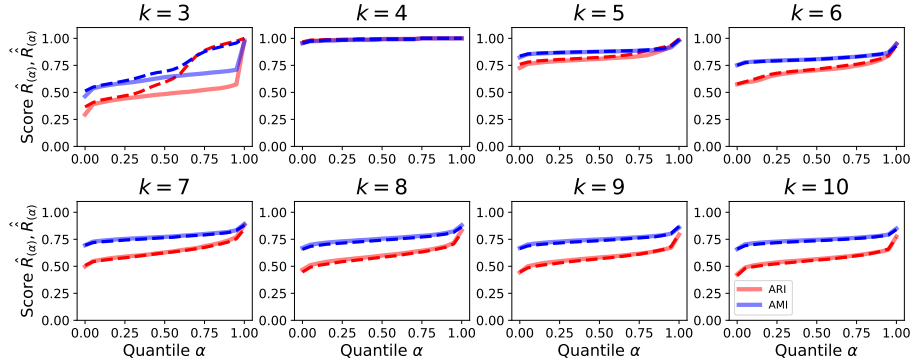


Figure 10: We use the same setup as Figure 8, now for data drawn from the distributions in Equation (10).

A.2 Replicability scores in the absence of clustering structure

To test whether our replicability metric is robust to the absence of clustering structure, we perform the following experiment. For fixed n , we draw $2n$ i.i.d. replicates x_1, \dots, x_{2n} from a fixed distribution F . We let $\mathbf{X} = [x_1, \dots, x_n]^\top$ and $\mathbf{X}' = [x_{n+1}, \dots, x_{2n}]^\top$ be the training and testing set respectively, and apply Algorithm 1 to inspect the behavior of the replicability scores on this data.

In our experiments below, we let F be the multivariate “standard” Gaussian, with mean the zero vector and covariance matrix the identity. In Figure 11 we fix

$d = 2$ and vary $n \in \{200, 350, 500\}$. The qualitative finding from both the ARI and AMI scores are reassuring: in both cases the scores are low, and uniform across different choices of k .

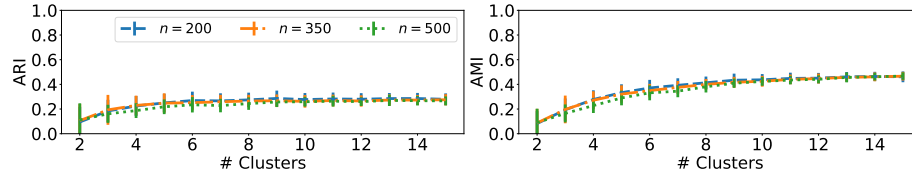


Figure 11: Replicability scores in the absence of clustering structure. We report the average replicability score \pm one standard deviation as obtained by $B = 100$ replicates according to Algorithm 1 (vertical axis, left: ARI, right: AMI) as we vary the number of clusters using k -means. Different line colors and styles refer to couples of training, testing datasets with different sizes n . Datapoints in the train and test dataset are i.i.d. multivariate Gaussian random draws with mean 0 and identity covariance matrix in \mathbb{R}^2 .

Next, we inspect the behavior of the replicability scores across different choices of the dimension d of the random vectors drawn — $d \in \{5, 10, 15\}$, to understand the role of dimensionality. Again, scores are low, and uniform across different choices of k . Here $n = 200$.

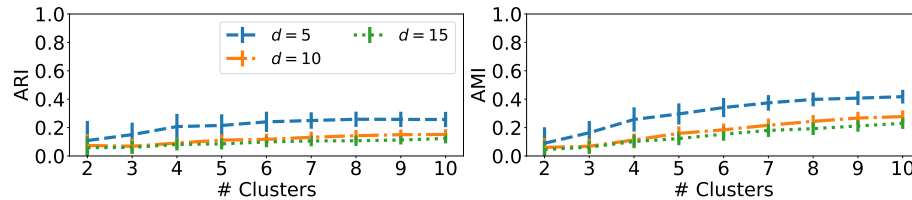


Figure 12: Replicability scores in the absence of clustering structure. We report the average replicability score \pm one standard deviation as obtained by $B = 100$ replicates according to Algorithm 1 (vertical axis, left: ARI, right: AMI) as we vary the number of clusters using k -means. Different line colors and styles refer to couples of training, testing datasets with different dimension d . Datapoints in the train and test dataset are i.i.d. multivariate Gaussian random draws with mean 0 and identity covariance matrix in \mathbb{R}^d . Here, $n = 200$.

A.3 The role of sample size in replicability metrics

The replicability measures defined in Section 3 depend on the sample sizes of the training and testing datasets. A simple example to explain why in our opinion this is appropriate, is as follows: consider a training dataset \mathbf{X} with n observations drawn i.i.d. from F_1 , and a testing dataset \mathbf{X}' with m observations drawn

i.i.d. from F_2 . For simplicity, let $n = m$, and F_1, F_2 be the same distribution (call it F), e.g. a mixture of Gaussians with a large number of well-separated components, say $k = 25$, with equal mixing weights over the components. When n is very small, e.g. $n = 50$, with high probability some of the components of F will be present in the training set, but absent in the testing set, and viceversa. We expect the replicability index to capture this phenomenon — in this case, for example, there might exist a value $k < 25$ which achieves a higher replicability score than $k = 25$. As n increases, however, with high probability both \mathbf{X} and \mathbf{X}' will contain datapoints from all components, and $k = 25$ will achieve the highest replicability score. We include a brief simulation experiment below — see Figures 13 and 14.

We emphasize that in applications with limited sample sizes, anticipating trends like the one discussed above is challenging, and it is not part of the aims of our manuscript. The focus is on replicability of the cluster analysis results with the available sample sizes, and not with hypothetical large sample sizes.

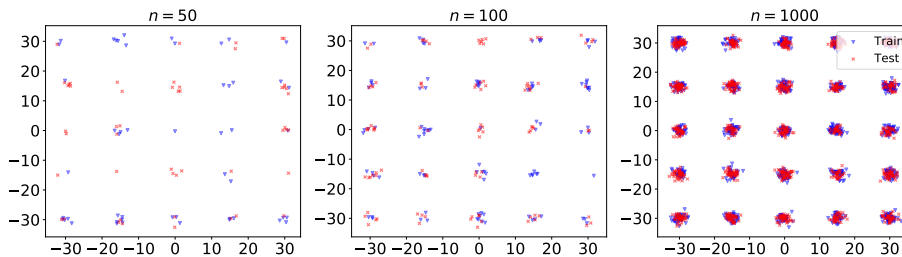


Figure 13: Three draws from a Gaussian mixture model in \mathbb{R}^2 with $k = 25$ well separated components. Left: $n = 50$, center: $n = 100$, right: $n = 1000$.

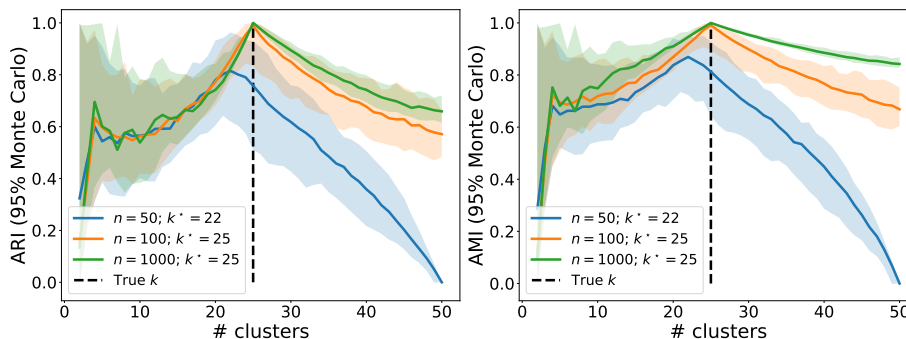


Figure 14: ARI and AMI replicability scores (vertical axis) across $N_{MC} = 100$ (Monte Carlo replicates) draws, for $n \in \{50, 100, 1000\}$, as the input parameter k of k -means varies (horizontal axis). For each n , we report the mean (solid line) when $m = n$, as well as centered 95% intervals across $k \in \{2, 3, \dots, 50\}$.

	Mainz	Transbig	Vdx
$\text{ARI}(\Pi_{\text{PAM50}}(\mathbf{X}), \Pi_{\text{3G}}(\mathbf{X}))$	0.33	0.34	0.53
$\text{AMI}(\Pi_{\text{PAM50}}(\mathbf{X}), \Pi_{\text{3G}}(\mathbf{X}))$	0.38	0.39	0.49

Table 1: Comparison of the subtype signatures for Mainz, Transbig and Vdx using either the three genes subset, or the PAM50 subset. For example, for the Mainz dataset, letting $\Pi_{\text{PAM50}}(\text{mainz})$ and $\Pi_{\text{3G}}(\text{mainz})$ be the PAM50 and 3G signatures (i.e. row-wise partitions) of the Mainz dataset, we compute $\text{ARI}(\Pi_{\text{PAM50}}(\text{mainz}), \Pi_{\text{3G}}(\text{mainz})) = 0.33$ and $\text{AMI}(\Pi_{\text{PAM50}}(\text{mainz}), \Pi_{\text{3G}}(\text{mainz})) = 0.38$.

B Additional figures and information about model-based signatures

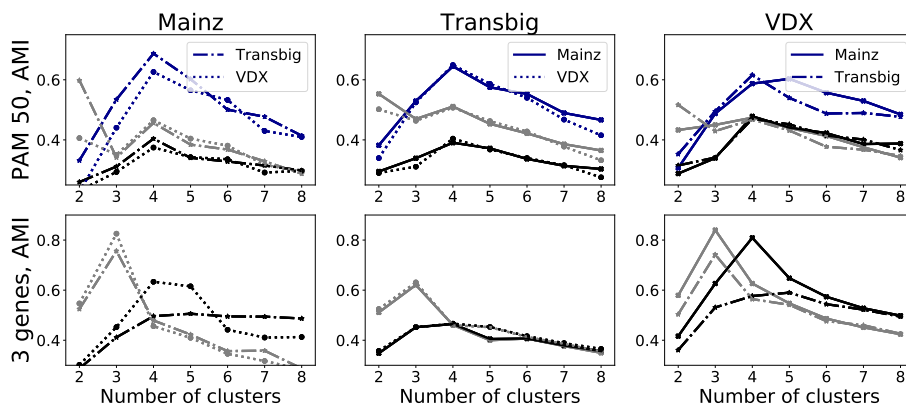


Figure 15: Each row refers to a different subset of genes (top row: PAM50 of Parker et al. [2009], bottom row: 3G of Haibe-Kains et al. [2012]). Each column refers to a different testing dataset \mathbf{X}' (left: Mainz, center: Transbig, right: VDX). For each gene subset, given testing dataset \mathbf{X}' , training dataset \mathbf{X} , algorithm \mathcal{A} and number of clusters k , we retain the partition $\Psi_{\mathbf{X}}^*(\mathbf{X}')$ with the highest replicability score across replications and compare it to known signatures $\Pi_{\text{PAM50}}(\mathbf{X}')$ (top row) and $\Pi_{\text{3G}}(\mathbf{X}')$ (bottom row) by computing $\text{AMI}(\Psi_{\mathbf{X}}^*(\mathbf{X}'), \Pi_{\text{PAM50}}(\mathbf{X}'))$ (top row – y -axis) and $\text{AMI}(\Psi_{\mathbf{X}}^*(\mathbf{X}'), \Pi_{\text{3G}}(\mathbf{X}'))$ (bottom row – y -axis).

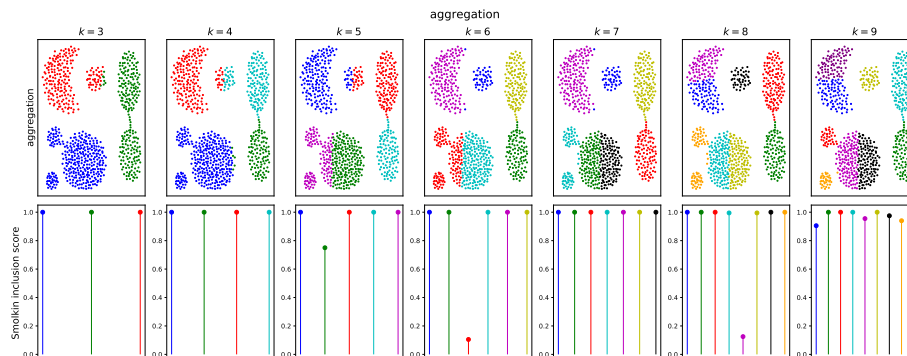


Figure 16: Smolkin-Ghosh inclusion score computed for the “aggregation” dataset using k -means, for different values of k .

C Methods from previous literature

In this section we provide experimental results for the competing methods described in Section 2. All code to replicate our experiments and reproduce figures is available at https://github.com/lorenzomasoero/clustering_replicability.

C.1 Clustering replicability via stability

Here we report results for the methods discussed in Section 2.2. We consider the datasets of Fränti and Sieranoja [2018].

C.1.1 Smolkin-Ghosh inclusion score

We start with the Smolkin-Ghosh inclusion score, proposed by Smolkin and Ghosh [2003] and described in Section 2.2.2. Since the datasets we consider are not very high-dimensional, we let $\alpha = 1$ in our experiments (i.e., retain all the covariates for the purposes of clustering). All our results are obtained by averaging over $B = 200$ bootstrap re-samples, using the k -means algorithm for different values of k . In Figures 16 to 18, we color-code in the first row the original clusters U_1, \dots, U_k obtained by running k -means. In the second row, for each cluster, we report the corresponding Smolkin-Ghosh inclusion score.

In our experiments using the Smolkin-Ghosh in Figure 16, we see that for $k = 3, 4, 5$, the replicability scores of all the clusters are close to 1 — the highest possible value. However, by visually inspecting the clustering learned, we notice that some of the clusters learned are spurious.

C.1.2 D Index

Next we consider the deletion (D) index, proposed by McShane et al. [2002] and described in Section 2.2.2. In Figures 19 to 21, we color-code in the first row the original clusters U_1, \dots, U_k obtained by running k -means. In the second

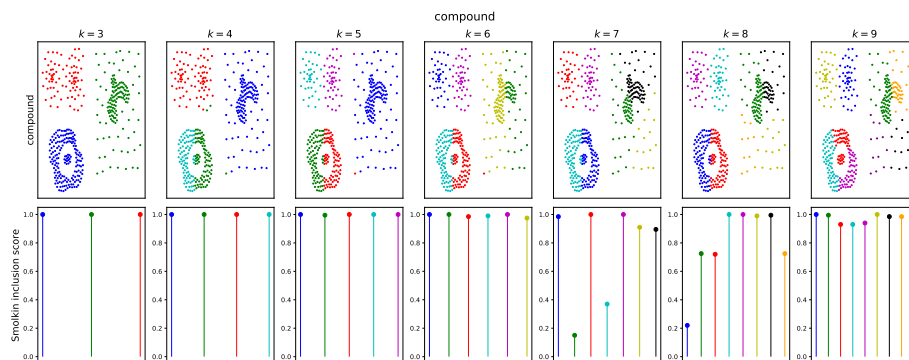


Figure 17: Smolkin-Ghosh inclusion score computed for the “compound” dataset using k -means, for different values of k .

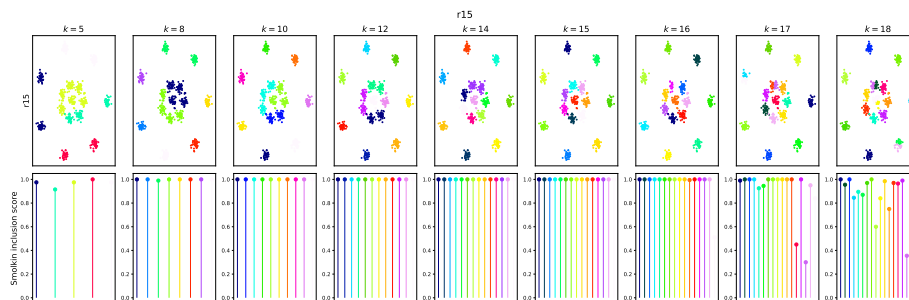


Figure 18: Smolkin-Ghosh inclusion score computed for the “r15” dataset using k -means, for different values of k .

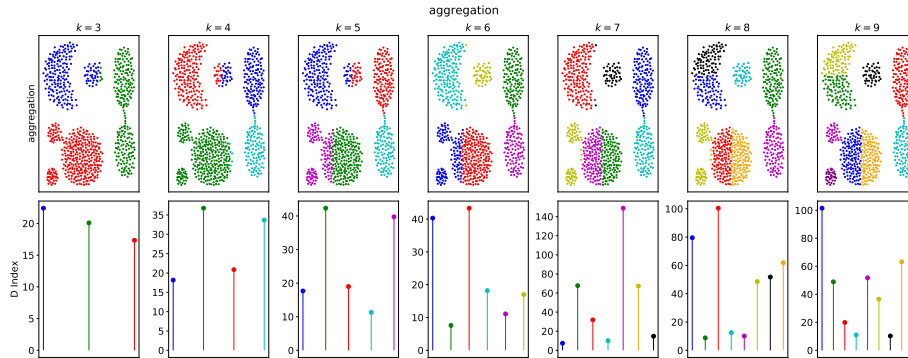


Figure 19: D index computed for the “aggregation” dataset using k -means, for different values of k .

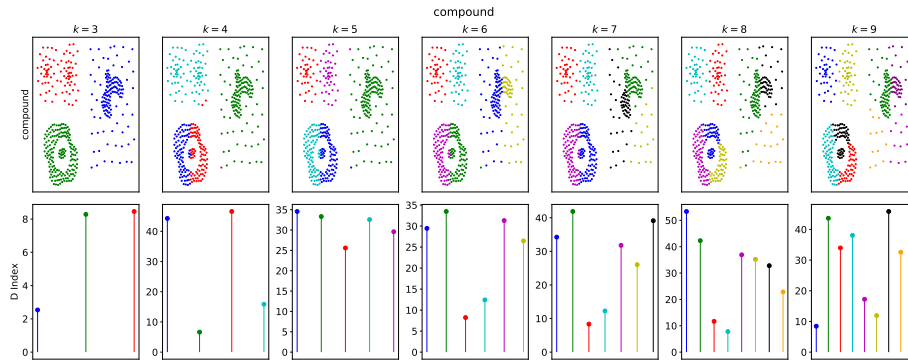


Figure 20: D index computed for the “compound” dataset using k -means, for different values of k .

row, for each cluster, we report the corresponding D index score obtained by clustering $B = 200$ perturbed versions of the original data. We perturb via additive Gaussian noise with variance given by $\hat{S}^2/2$, where \hat{S}^2 is the sample variance for the dataset under consideration (i.e., the n -th point in the b -th perturbed dataset is given by $\tilde{x}_n = x_n + e_n^{(b)}$, with $e_n^{(b)} \sim \mathcal{N}(0, \hat{S}^2)$).

In our experiments, we find that the D index can be useful to identify spurious clusters. One limitation of the score is that — as is — the D index provides an (average) absolute number of deletions per cluster over the random re-samples. This can make the stability comparison between different clusters unfair, especially if their sizes are unbalanced. Therefore, we believe that reporting the average *relative* number of deletions (with respect to the original cluster size) over the random re-samples allows for a more direct and effective comparison of the stability of clusters.

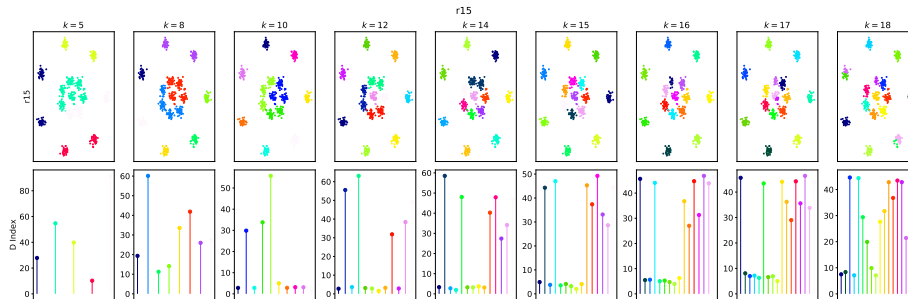


Figure 21: D index computed for the “r15” dataset using k -means, for different values of k .

C.1.3 R Index

Next we consider the R index, proposed by McShane et al. [2002] and described in Section 2.2.2. In Figures 22 to 24, we color-code in the first row the original clusters U_1, \dots, U_k obtained by running k -means. In the second row, for each cluster, we report the corresponding R index score obtained by clustering $B = 200$ perturbed version of the original data. We perturb via additive Gaussian noise with variance given by $\hat{S}^2/2$, where \hat{S}^2 is the sample variance for the dataset under consideration (i.e., the n -th point in the b -th perturbed dataset is given by $\tilde{x}_n = x_n + e_n^{(b)}$, with $e_n^{(b)} \sim \mathcal{N}(0, \hat{S}^2)$).

In our experiments, we find that the R index can be a useful metrics to identify which cluster is more stable among the ones found. We also find that, in certain instances, the value of the score can be misleading. For example, in Figure 22, for $k = 5$, while the algorithm fails to effectively identify well separated clusters, the R scores are not particularly low. This might lead to interpretability issues in high dimensional settings. As a side note, the findings of the R and D index heavily depend on the specification of the variance of the noise. We recommend running sensitivity analyses and carefully choosing this parameter when running analyses based on these indices.

C.2 Clustering replicability via prediction accuracy

Here we report results for the methods discussed in Section 2.3. Again, we consider the datasets of Fränti and Sieranoja [2018].

We start by providing results for the prediction strength introduced by Tibshirani and Walther [2005] for the three datasets already considered in the previous section. Results are reported in Figure 25. One of our findings — consistent across our experiments — is that the prediction strength tends to favor the choice of fewer clusters, even when such choice does not result in a better clustering. This is due to the fact that the prediction strength is obtained by applying the minimum operator across a cluster-specific score (see Equation (4) in the main manuscript [Masoero et al., 2022a]). Practitioners using the prediction score

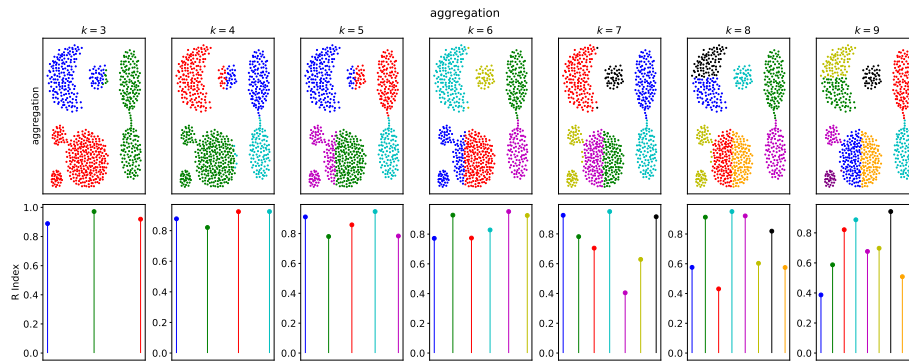


Figure 22: R index computed for the “aggregation” dataset using k -means, for different values of k .

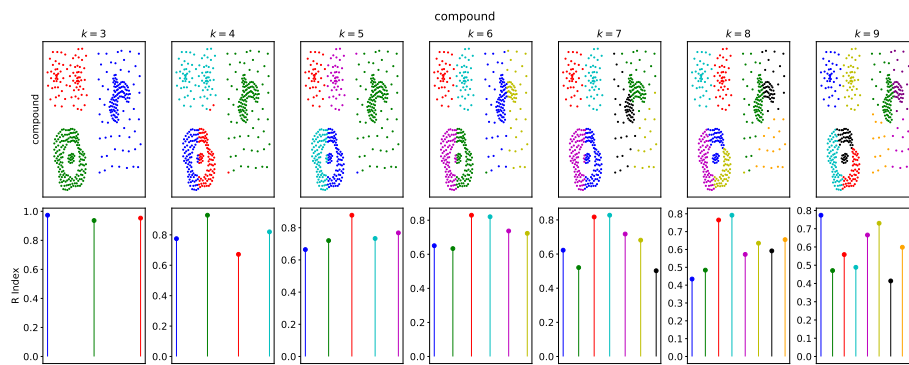


Figure 23: R index computed for the “compound” dataset using k -means, for different values of k .

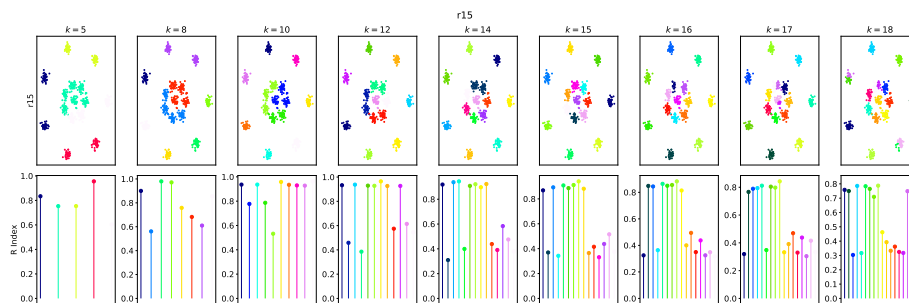


Figure 24: R index computed for the “r15” dataset using k -means, for different values of k .

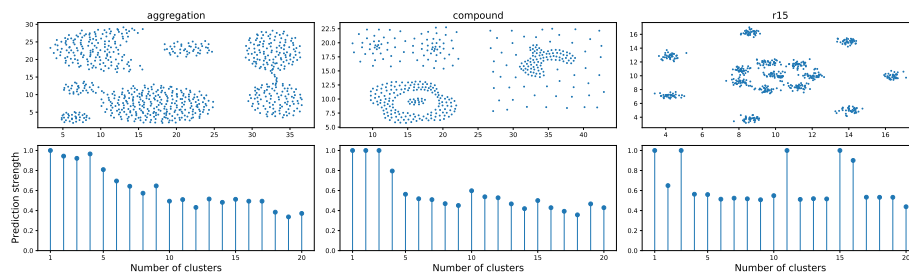


Figure 25: Prediction strength computed for the “aggregation”, “compound” and “r15” datasets using k -means, for different values of k .

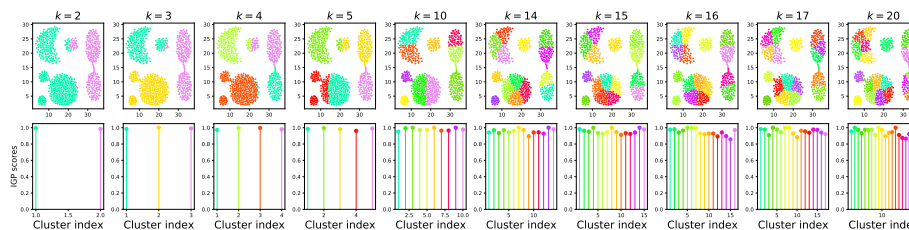


Figure 26: IGP computed for the “aggregation” dataset using k -means, for different values of k .

as a diagnostic tool to assess clustering replicability should be cautious and aware of this feature. We suggest monitoring all the cluster-specific scores that are contained inside the min operator in Equation (4) in the main manuscript [Masoero et al., 2022a] to better understand the performance of the clustering algorithm at a global scale.

Next, we provide results for the IGP, first proposed in Kapp and Tibshirani [2006], in Figures 26 to 28. In our experiments, we find that the IGP scores tend to provide an overconfident statement about the replicability of clustering algorithms, often providing scores close to 1 (the highest possible value) also for spurious clusters (see, e.g., the case of $k = 10$ for the “aggregation” dataset in Figure 26). We notice that both the prediction strength and the IGP do not require the specification of any additional parameter to assess replicability other than the choice of the clustering algorithm. In applications, it might be good practice to compute these scores on the original dataset as well as on perturbed versions of the original data, in a similar fashion to what is performed to obtain the D and R indices. Moreover, for the IGP, we suggest practitioners interested in using this metric to not only compute the metric using only each point’s nearest neighbor, but also other points nearby (e.g., compute the score by checking whether all j -nearest neighbors belong to the same cluster, for different values of j).

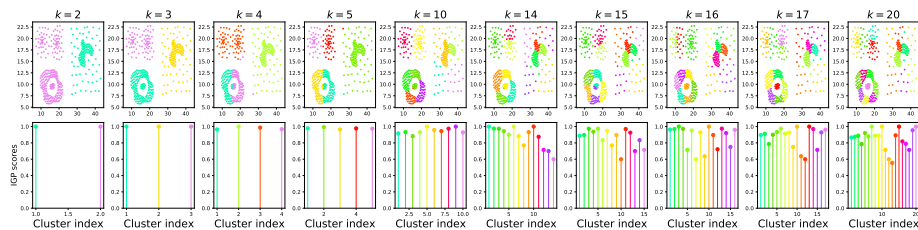


Figure 27: IGP computed for the “compound” dataset using k -means, for different values of k .

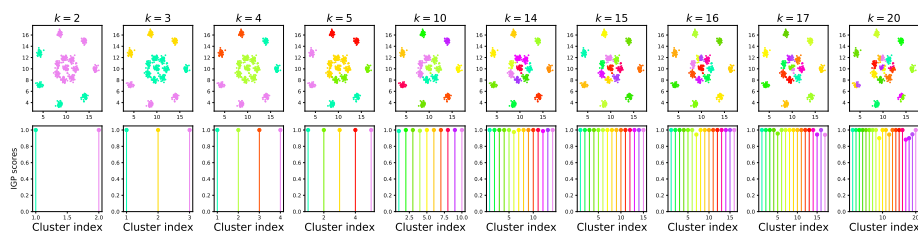


Figure 28: IGP computed for the “r15” dataset using k -means, for different values of k .

C.3 Clustering replicability via tests of significance

Last, we discuss replicability metrics that rely on significance tests as discussed in Section 2.4. In particular, we follow the procedure proposed by McShane et al. [2002] and report results obtained on synthetic data in Figures 29 and 30.

First, in Figure 29, we draw $N = 1000$ samples from Gaussian mixture models in \mathbb{R}^2 with k components, for $k \in \{1, 2, 3, 5\}$. The data is plotted in the first row of the figure. For each of these datasets, we test the null hypothesis H_0 of absence of clustering following the procedure discussed in Section 2.4, using a multivariate Gaussian distribution with mean given by the sample mean and covariance matrix given by the sample covariance matrix to draw from the null model. In our simulation, we let $B = 200$ (i.e., we redraw $B = 200$ datasets of size $N = 1000$, and for each $b = 1, \dots, B$ of these datasets compute the score s_b discussed in Section 2.4. Results (and corresponding p -value under the null) are reported in the second row of the figure. The test behaves as expected — in particular, it successfully allows to reject the null hypothesis when a clear clustering structure is present in the data.

Next, we analyze the sensitivity of the test as a function of the separation between the clusters in the data. Towards this goal, we consider $N = 1000$ datapoints drawn from balanced bi-variate Gaussian mixture models in \mathbb{R}^2 ,

$$F = \frac{1}{2}\mathcal{N}(\mu_1, I) + \frac{1}{2}\mathcal{N}(\mu_2, I).$$

We analyze how the test behaves as we decrease the distance between the means of

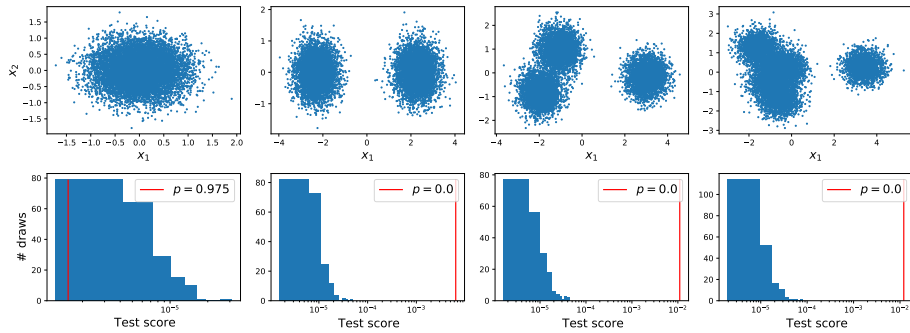


Figure 29: Statistical tests of significance to reject the null hypothesis H_0 that no clustering structure is present in the data.

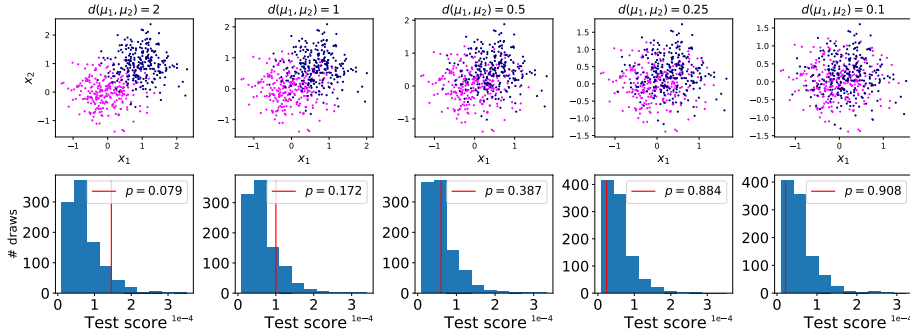


Figure 30: Statistical tests of significance to reject the null hypothesis H_0 that no clustering structure is present in the data.

the two components μ_1, μ_2 . Results are reported along the columns of Figure 30. As expected, as we decrease the distance, and the clustering structure becomes less clear, the p -value associated with the test starts decreasing. For ease of visualization, we color points belonging to different clusters with different colors.